Centrifugal and Numerical Investigation of Surface Fault Rupture Hazard Mitigation for Shallow Foundations Using Micro-Piles

Alireza Saeedi Azizkandi (asaeedia@iust.ac.ir)
Iran University of Science and Technology https://orcid.org/0000-0003-2924-9443
Sheida Majidi
Iran University of Science and Technology
Sadegh Ghavami
Iran University of Science and Technology

Research Article

Keywords: reverse fault rupture, mitigation strategy, centrifuge modeling, 3D finite element analysis, stiff inclined micro-piles

Posted Date: February 15th, 2021

DOI: https://doi.org/10.21203/rs.3.rs-222418/v1

Centrifugal and Numerical Investigation of Surface Fault Rupture Hazard Mitigation for Shallow Foundations Using Micro-Piles

Alireza Saeedi Azizkandi [1], Sheida Majidi [2], Sadegh Ghavami [3]

[1] Assistant Professor, School of Civil Engineering, Iran University of Science and Technology, Tehran, Iran. (corresponding author). Email: asaeedia@iust.ac.ir ORCID: https://orcid.org/0000-0003-2924-9443

[2] School of Civil Engineering, Iran University of Science and Technology, Tehran, Iran. Email: sheida_majidi@cmps2.iust.ac.ir ORCD: https://orcid.org/0000-0002-5163-2556

[3] School of Civil Engineering, Iran University of Science and Technology, Tehran, Iran. Email: s_ghavamijamal@civileng.iust.ac.ir ORCID: https://orcid.org/0000-0001-5102-7658

Abstract

Surface fault rupturing mostly contributes to either large-scale destruction or minor damage of the constructions and the infrastructures which are built across fault zones. Among the numerous mitigation strategies which have been suggested, a novel approach refers to implementing expanded polystyrene sheets (EPS) wall to deviate the fault rupture. However, the shallow foundations which are protected by EPS walls still rotate in some particular positions toward the fault rupture. This study investigates the probability of deviating the reverse fault rupture by installing a strong inclined wall (SIW) beneath the surface foundation both physically and numerically. Due to the effectiveness of adopting the mentioned method, a further three-dimensional (3D) finite-element (FE) modeling is conducted, employing the validated numerical model to divide the SIW into a row of strong inclined micro-piles (SIMPs). The installation of SIMPs in both a convenient and environmentally friendly strategy was carried out and the pivotal parameters of designing such micro-piles including their diameter, the angle of installation, and the optimal distance between each two-consecutive implemented micro-piles were investigated in a parametric study. The results indicate that executing a well-designed row of micro-piles with the proper angle of installation can protect a surface foundation against a reverse fault rupture.

Keywords: reverse fault rupture, mitigation strategy, centrifuge modeling, 3D finite element analysis, stiff inclined micro-piles

Introduction

The consecutive occurrence of earthquakes that were associated with surface fault rupture and the various consequences of their detriments have made earthquake engineers conduct comprehensive surveys on practical approaches to reduce the fault rupture risk on the surface foundation by deviating the earthquake fault. Precise investigations of survived cases during the recently-happened fault rupture and examining them end up arising an interdependence phenomenon that is termed FR-SFSI (Fault Rupture- Soil- Foundation- Structure Interaction). Researches on the FR-SFSI subject can be broadly categorized into three groups: (i) analyzing the case histories of surface faulting (Kelson et al., 2001; Anastasopoulos and Gazetas, 2007; Faccioli et al., 2008), (ii) physical modeling (Bray, 2001; Lee et al., 2005; Bransby et al., 2008a,b; Chang et al., 2013), (iii) numerical modeling (Loukidis and Bouckovalas, 2001; Yilmaz and Paolucci, 2007; Anastasopoulos et al., 2007, 2010; Baziar et al., 2012). Field studies as the first approach among voluminous literature on this field have been mostly done after three major earthquakes:

The M_w 7.4 Kocaeli earthquake (1999), the M_w 7.1 Duzce earthquake (1999) which both of them happened in Turkey, and the M_w 7.6 Chi-Chi (1999) which was occurred in Taiwan. During the mentioned earthquakes, it was observed that despite the huge amount of damages, some of structures whose foundations rested on either box-type foundations or rigid ones, have not only remained without any serious detriments, but also caused deviation of fault rupture due to their heavily loaded surface foundation (Anastasopolous and Gazetas 2007a,b). Fig. 1 and 2 both depict the main features of two such examples. In Fig.1, a 4-storey reinforced concrete building plus basement, resting on a continuous rigid box-type foundation which survived from downward dislocation of 2.3 m without any substantial structural damages. Due to the 2.3 m of subsidence, its basement was immersed in the water table and the flooding spoiled it (Anastasopolous and Gazetas, 2007). Meanwhile, another 4-storey reinforced apartment is depicted in Fig.2, its continuous and rigid foundation has undergone about 10° rotation and an approximate upthrust of 4 m, though the building has remained without any severe damage (Faccioli et al., 2008). Moreover, it can be perceived that both of these mentioned buildings effectively diverted the surface ruptures' path (Faccioli et al., 2008; Anastasopolous et al., 2008). Turning to physical modeling investigations, centrifuge model experiments are widely used to develop a profound understanding of mechanisms. Anastasopolous et al. (2007) by using centrifugal experiments concluded that due to the tensile failure of the piles at their tops, the piled-foundation buildings are inefficient in comparison with the ones on a rigid and continuous foundation. Moreover, with the help of centrifuge tests, other key parameters in the durability of a structure subjecting to either normal or reverse fault rupture were investigated. These critical parameters can be listed as bearing pressure and the relative position of the fault to the foundation and how heavily a foundation is loaded (Bransby et al., 2008). Numerical investigations as an inexpensive and convenient method have mainly been used by a great number of scholars to scrutinize other possible key factors of mitigation fault hazards. Lin et al. (2006), who evaluated the effects of parameters in deformation behavior, illustrated that young's modulus, dilation angle of the soil, and dip angle of the fault play a crucial role in determining fault rupture.

Due to both the inevitability of constructing in fault zones and the uncertainty in specifying the rupture zone, various mitigation categories have been suggested so far which can be classified into two distinct categories: (i) strengthening the foundations (Bray, 2001; Gazetas et al., 2008; Faccioli et al., 2008), and (ii) deviating fault rupture (Fadaee et al., 2013; Oettle et al., 2013). Strengthening foundation as the former strategy can be applied just by building the foundation in the form of a rigid body. Although strengthening foundations prevents structures from total collapse, the rotation of the structure is inescapable and correspondingly, the structure subjected to fault rupture would be non-functional (Fadaee et al., 2016). Therefore; the latter approach as a more rational strategy and capable of applying to both new and existing buildings contributes to many surveys that have been conducted to figure out how to deviate fault rupture and reduce the foundations' rotation. To make the fault deviated and at the same time to equip the foundation with fewer rotations, Oettle and Bray (2013) investigated the efficiency of geotechnical mitigation methods through the latter approach (deviating fault ruptures) using a robust diaphragm wall between the foundation and the bedrock fault to deflect fault rupture. However, implementing a diaphragm wall might not be always regarded as the best solution due to the high relevancy of the diaphragm wall's efficiency with the exact place of faults. Adversely, a weak wall barrier consists of soil and bentonite was modeled by Fadaee et al. (2016) to divert the fault rupture. Such Soil-Bentonite wall (SBW) demonstrates great capability due to its low strength and stiffness. However, the shear strength of the soil is heavily dependent on time and will be intensified as time marches on which can be considered as a weak-point for this method. In a parallel approach, Ashtiani et al. (2017) studied the usefulness of other materials to be implemented as a trenching wall to divert fault rupture. Among the materials which they used, expanded polystyrene foam sheets (i.e. EPS) as a material neither with high shear strength nor being dependent on time exhibited the best performance in deviating fault rupture. Baziar et al. (2019) numerically considered the efficiency of trenching an EPS wall in a proper situation to a surface foundation against reverse fault rupture, which indicated that besides EPS wall's geometry, some parameters like foundation position (S) and fault dip angle (α), play a crucial role in the effectiveness of their strategy. They concluded that, although an EPS wall performed favorable results to mitigate fault rupture in many various positions of surface foundation (Table.1), some locations have still stayed in a threatening damage level with high rotations. These critical positions are more comprehensively shown in Table.2, where the parameter "S" illustrates the distance between the left corner of the foundation and the place where the free-field rupture crosses the base and the parameter "B" indicates the width of the foundation. Therefore, the important question remains: what can be done in the case where a weak vertical wall is ineffective due to not being possible to deviate the fault rupture?

Table. 1. Summary of protectable positions for a shallow foundation with EPS wall mitigation (Baziar et al. 2019)

0 ≤ Rotation (θ) < 1		2 ≤ Rotation (θ) < 5			5 ≤ Rotation (θ)		
Position / dip angle	S/B = -0.25	S/B = 0	S/B = 0.25	S/B = 0.5	S/B = 0.75	S/B = 1	S/B = 1.25
60							
75							

Table 2. Summary of critical protected positions for surface foundations with EPS wall mitigation (Baziar et al. 2019)

0 ≤ Rotation (θ) < 1	2 ≤ Rotation (θ) < 5		5 ≤ Rotation (θ)
Position / dip angle	S/B = -0.25	S/B = 0	S/B = 0.25
60			
75			

This paper will thoroughly focus on the effectiveness of trenching a strong inclined wall (SIW) beneath the surface foundation to decrease the foundation's rotation when it is located at the critical positions (Table.2), to solve the weaknesses of conducting a weak vertical wall. The efficiency of the mentioned SIW was examined both experimentally using centrifuge modeling and numerically using 2D and 3D finite element method. Afterward, to enhance the installation procedure, a novel approach has been proposed to divide the SIW into a row of strongly inclined micro-piles (SIMPs). The practicality of driving a row of micro-piles besides a surface foundation to deviate the fault rupture path was examined numerically. Lastly, the influential parameters to gain a well-design and well-adjusted row of inclined micro-piles to protect a surface foundation against a reverse fault rupture were numerically discussed. Although the possibility of fault rupture can be dependent on various parameters such as the thickness of the sand layer and the location of fault with respect to fault rupture on the soil-rock interface (Anastasopoulos et. al, 2008; Paolucci and Yilmaz, 2008), in this study, to solve the weaknesses of trenching a weak vertical wall in some specific conditions, and with regards to the effectiveness of trenching a strong inclined wall to deviate the fault rupture, parametric studies of strongly inclined micro-piles (SIMPs) were chosen in a way to make the most out of trenching SIMPs. Such parameters include the diameter of micro-piles, the angle of their installation, the distance between every two consecutive micro-piles, all of which have been investigated to protect a surface foundation that is affected by reverse fault rupture of both 60- and 75-degree.

The organization of this paper is as follows. In Section Two, the experimental modeling of a SIW is carried out by using centrifuge tests which simulate a reverse fault of dip angle 75 through a dry sand layer at 50 times Earth's gravity. In section Three, both the free-field centrifuge model and the one when the foundation is positioned at (S/B=0) with the mitigating element are validated through the finite element modeling approach. Furthermore, finite element code ABAQUS is used to evaluate the feasibility of conducting a row of strongly inclined micro-piles which are divided from the experimented inclined wall. In Section Four, a parametric study is set out to optimum the rotation of foundation by finding the best parameters' quantities of micro-piles. It should be mentioned that the method which has been proposed is considered as a kind of novelty to mitigate the fault rupture. Finally, in Section Five, the main conclusions of this study will be presented.

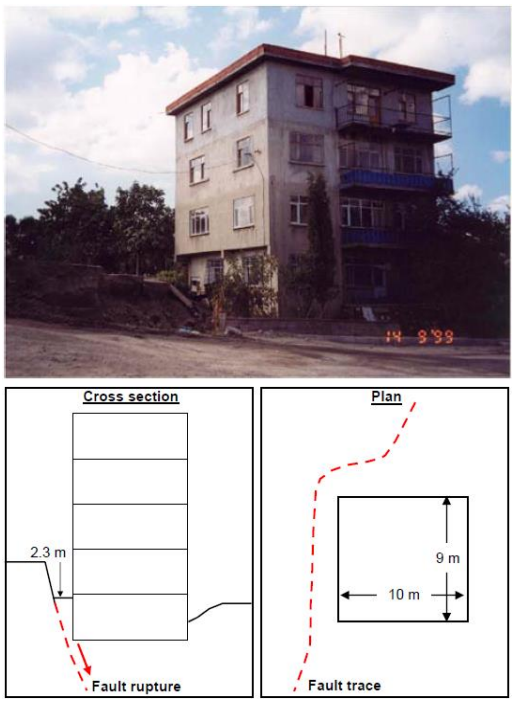

Fig. 1. Normal fault east of Golcuk, Kocaeli, Turkey 1999 earthquake – Denizevler: 4-storey building with basement resting on the continuous and rigid box-type foundation. (Faccioli et al. 2008)

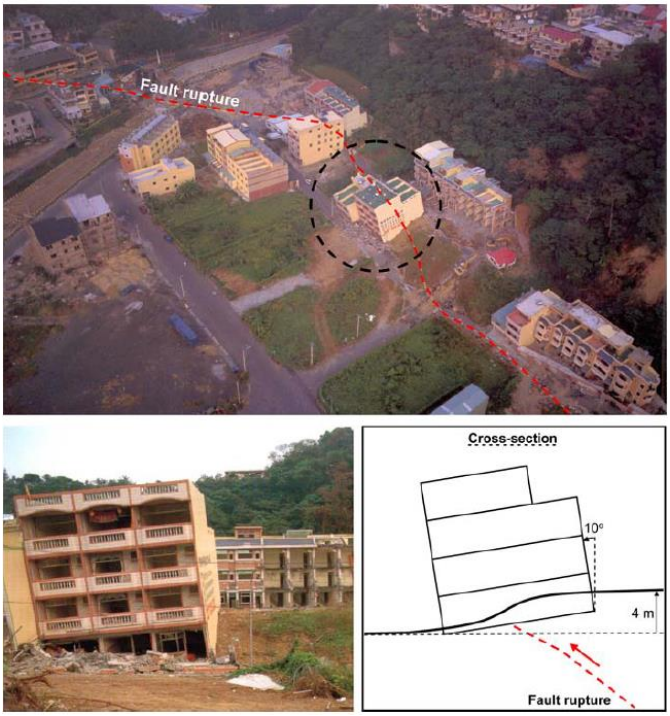

Fig. 2. Chelungpu thrust fault Chi-Chi, Taiwan 1999 earthquake – Chung-Cheng Park, Fung-Yan city: 4-storey building resting on a continuous and rigid foundation (photos adopted from Hwang 2000) (Faccioli et al. 2008)

Problem Definition and Methodology

Baziar et al. (2019) indicated that installing a weak vertical wall (WVW) can deviate the fault rupture; hence, protect the surface foundation. However, since the effectiveness of such WVW heavily depends on the foundation's location, in certain positions, the surface foundation remains unprotected (Table. 2). Therefore, to ameliorate the mentioned situations, trenching a strong inclined wall (SIW) beneath the foundation, filled with concrete, is proposed as a useful approach in diverting the fault trace. A series of physical experiments using centrifuge were done to prove the theory and were followed by finite element numerical modeling, verified by the test results. Due to the effectiveness of implementing a SIW to mitigate fault rupture and protect the surface foundation, we introduce a row of strongly inclined micro-piles (SIMPs) which are subdivided from the mentioned wall with different constructing and locating features. The effectiveness of such a group of micro-piles seems to have a direct connection with the fault dip angle (α), angle of installation of the group of micro-piles, the distance between installed micro-piles with each other, and the diameter of micro-piles, commensurately. As schematically illustrated in Fig.3, the studied problem subjecting to a reverse fault of dip angle α (which in this paper, α has been assumed as both 60degree and 75degree), producing an upward displacement of vertical amplitude h, propagating through a uniform soil deposit with the thickness of 12m. The rotation of a surface foundation with a width of 8.5m carrying a surcharge load of 81 kPa locating at S/B=0 was investigated while a row of SIMPs was installed just in 0.5 m distance (from the center of micro-piles) toward the left side of the surface foundation. The mentioned parameters in Fig.3 including the angle of inclined micro-piles, distance between consecutive micro-piles, and the diameter of micro-piles were numerically examined using ABAQUS (2014).

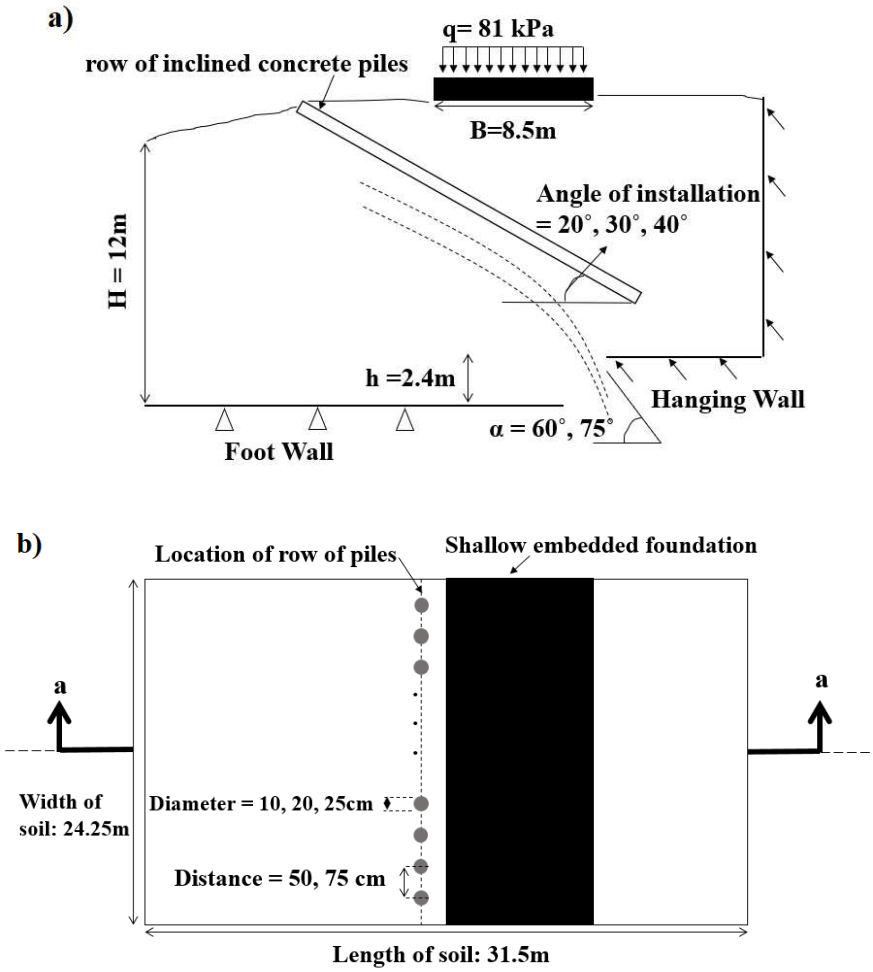

Fig. 3. Schematic representation of the investigated problem; (a) the row of micro-piles suggested subdividing from the inclined concrete wall, (b) cross-section a-a of the 3D finite element discretization, showing the place of micro-piles and the parameters which were investigated.

Physical Modelling

Physical modeling is employed to investigate the efficiency of trenching an inclined wall to deviate fault rupture. Fig.4 illustrates the apparatus of the centrifuge model used for this. As it is clear, the centrifuge consisting of a beam centrifuge with a free-swinging basket was used to simulate the fault ruptures in the centrifuge facility of the University of Tehran. Tests were conducted undergoing 50-g (the Earth's gravity) centrifugal acceleration. The split box was designed and constructed to simulate reverse fault of dip angle 75° in the centrifuge, with outer dimensions of 100 cm length, 50 cm width, and 34 cm height. A hydraulic jack was used at the bottom of the box to simulate the hanging wall when a reverse fault occurs by making a part of the bottom moveable. This hanging wall was designed with 20 cm length, and the maximum allowable offset of the fault with the 75° dip angle was 5 cm (2.5m at 50-g centrifugal acceleration). One side of the whole apparatus was equipped with Plexiglas, providing observation with the ability to compute the deformation through image analysis.

A clean uniform fine-grained Sand No.161 Firoozkuh was used in centrifuge experiments. The other properties of the Firoozkuh No.161 except what is shown in Table.3 are the relative density of 60%, moisture content of 5%, and corresponding to a unit weight of Υ_{wet}=16.05 kN/m^3 (Ashtiani et al., 2016). The layering of the mentioned sand was done in layers with a thickness of approximately 3 cm which each layer was compacted homogeneously using a calibrated steel hammer when the layer is poured. Moreover, after compression of each layer, a thin dyed blue sand was deposited tangent to the Plexiglas window in terms of making the fault rupture more highlight among the soil. The total layers of the sand consist of a thickness of 20 cm, which would be 12 m at prototype scale.

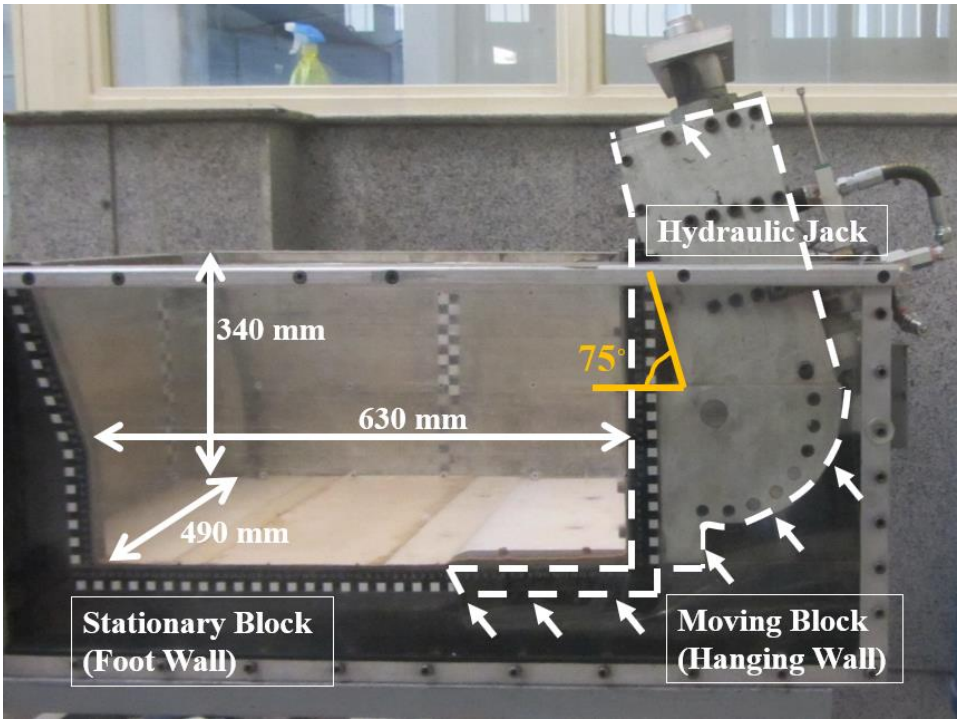

Fig. 4. Centrifugal fault rupture simulation apparatus and its dimension

Table 3. Summary of soil properties used for both physical and numerical experiments.

Name	D_{50} (mm)	e_{max}	e_{min}	γ_{wet} (KN/m^3)	ϕ_p (degree)	$\phi_{residual}$ (degree)	Ψ_p (degree)
Firoozkuh Sand No. 161	0.3	0.943	0.603	15.77	33	31	1

For this study, two centrifugal tests under 50-g centrifugal acceleration were performed. Firstly, the free-field test was conducted to observe the fault rupture path as well as determine the "S" parameter which depicts the relative situation of the foundation toward the fault rupture. According to the results of research conducted by Baziar et al. (2019), the foundation positioned at S/B=0 related to the fault surface outcrop has high rotation. Therefore, the second test was performed to investigate the mitigation of fault rupture hazard on this foundation. For this purpose, a strong inclined wall was used under the foundation. Once the embankment was done similar to the non-mitigated test, excavation was conducted to a favorable location. Then, a plate made up of aluminum with an angle of $\beta = 36°$ (with horizontal axis), was embedded in the soil, and the embankment of sand layers was done as before. To implement a well-designed reduced-scale model of each pile, wall, and other structures similar to the prototype, it is of paramount importance to make the bending stiffness (EI) of them equivalent using the following equation:

$$E_m I_m \times N^4 = E_p I_p \qquad (1)$$

Where N is gravity level in the centrifuge tests, E is Young's modulus of the model, E_p is Young's modulus of the prototype, I_m is the cross-sectional moment of inertia of the model, and I_p is the cross-sectional moment of inertia of the prototype. According to Eq. (1), an aluminum plate with dimensions of 490 × 300 × 4 mm (width × length × thickness), combined with Young's modulus of 70 GPa was embedded in the soil during the centrifugal test to simulate a concrete inclined slab wall of 15 × 0.56 m (length × thickness in prototype) with Young's modulus of 25 GPa. To put it in other words, to simulate the prototype concrete material, a model section made of a different material or aluminum was used (Hayward e al. 2000; Abdoun et al. 2003; Knappett and Madabhushi, 2009; Azizkandi et al. 2019; Baziar et al. 2020). Such simulation was used before, by Choo et al. (2010) and Zeping et al. (2014), when an aluminum plate was implemented to model the bending stiffness of the prototype concrete face in the concrete-faced rock-fill dam. At the top of soil including the inclined wall, a surface foundation made up of a rigid steel plate with a breadth of B=170 mm (8.5m at prototype scale) and thickness of t=21 mm (1.05 at prototype scale) was placed at the position of S/B=0. This rigid foundation subjecting to a fault rupture of 75° dip angle can generate bearing pressure of q= 81 kPa which can represent an 8-storey building with a minimum value of 10 kPa per story (Fig.5). The schematic picture of the problems investigated in the centrifuge is shown in Fig.6.

During the centrifuge testing, movement and rotation of the surface foundation were monitored using three linear variable displacement transducers (LVDTs) whose locations are shown in Fig. 6.b. To monitor the progress of the reverse fault offset, another LVDT was also placed on the hydraulic jack of the centrifuge. Particle Image Velocimetry (PIV) was used to measure soil deformation, and the GeoPIV software was also used to analyze the digital images of the soil sample (White et al. 2003).

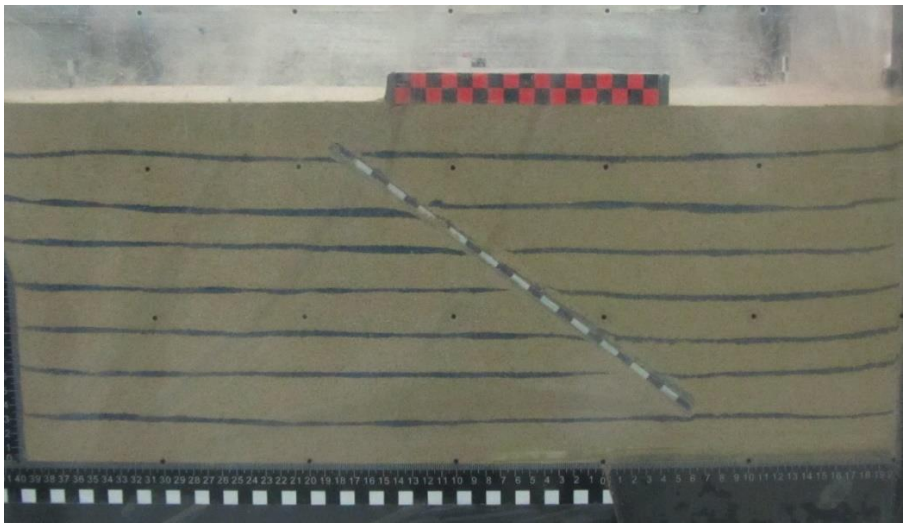

Fig. 5. Centrifuge model inside the spilt box including both surface foundation and strong inclined wall

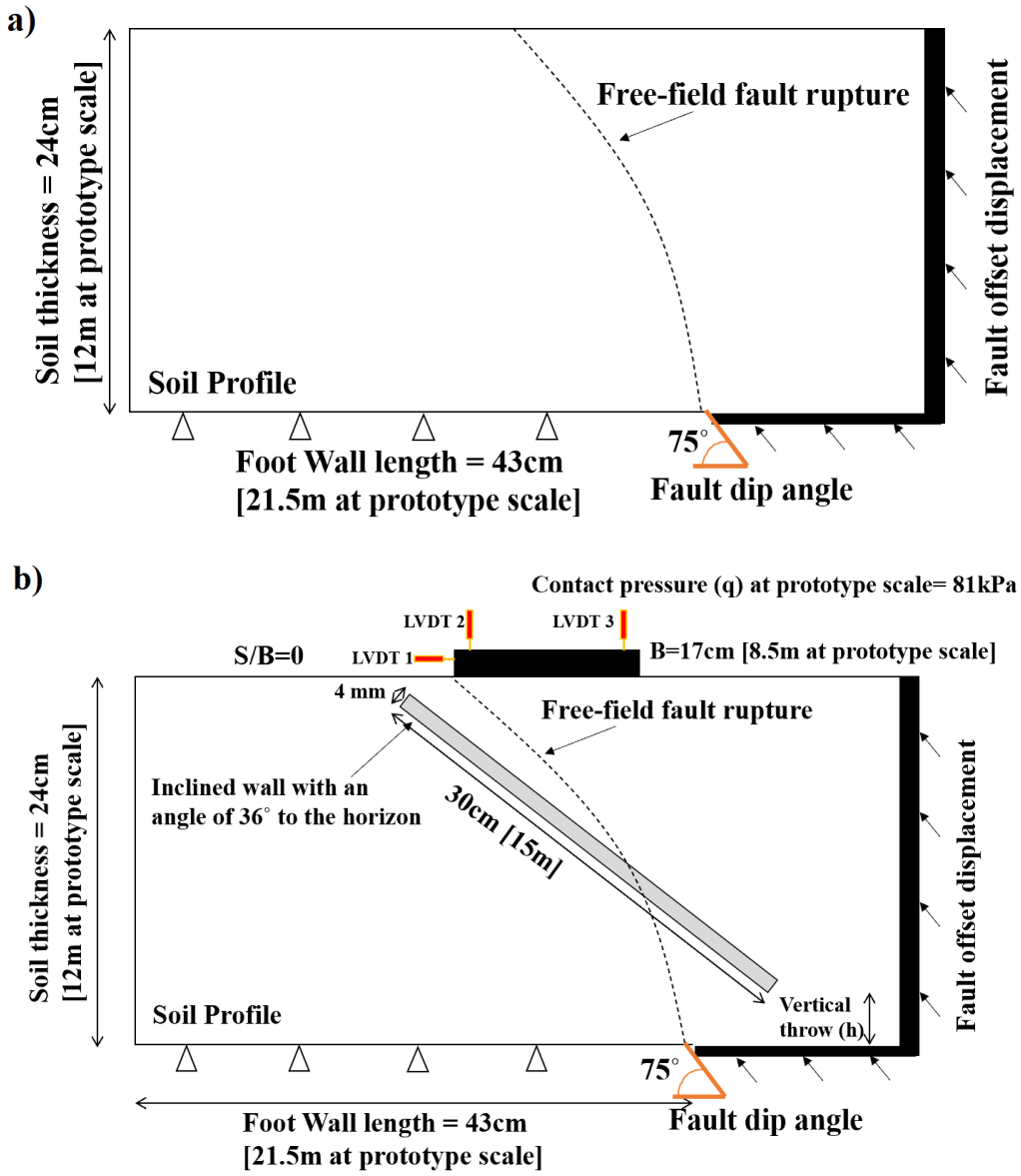

Fig. 6. Schematic view of centrifuge experiments; (a) First test conducted to observe the free-field fault rupture, (b) second test to observe the practicability of implementing an inclined wall

Finite Element Modelling and Validation

It has been shown that the finite element (FE) modeling can be considered as the most effective approach to reproduce both fault rupture propagation in the free-field and the interaction between fault rupture and surface foundation (Anastasopoulos et al., 2009). Finite Element coding with a hyperbolic nonlinear elastic constitutive law was used by Bray (1991) and Bray et al. (1994), which indicated satisfactory agreement between the experimental and numerical results. White (1994), Nakai et al. (1995), Erickson et al. (2001), and Loukidis et al. (1999) all used a Finite Difference (FD) software through implementing an elasto-plastic Mohr-Coulomb failure criterion and strain softening. Hence, according to the mentioned published research, both FE and FD methods can be successful in simulating fault rupture propagation through the soil. Bray et al. (1994a) indicated that providing some certain conditions such as a refined mesh in the vicinity of the potential fault rupture and a nonlinear constitutive law for the soil can make FE modeling successful. Also, Anastasopoulos et al. (2007) used an elasto-plastic Mohr-Coulomb constitutive model with isotropic

strain softening, using a Finite Element (FE) analysis, which was introduced by reducing the mobilized friction angle φ_{mob} and the mobilized dilation angle Ψ_{mob} by increasing the octahedral plastic shear strain γ^p_f. Ashtiani et al. (2015) carried out several direct shear tests on soil samples with the relative density of $D_r = 60\%$ (providing relatively loose sand) and moisture content of 5% which resulted in peak and residual friction angles of $\varphi_p = 33°$ and $\varphi_{res} = 31°$, respectively, and peak dilation angle of $\Psi_p = 1°$ for stress at mid-depth of the sand layer in the centrifuge test. They also numerically considered the strain-softening effect and found that using the strain-softening model changed the results just above 5% while substantially increased the run times of modeling. Therefore, despite the inevitable accuracy of results for dilative soil through conducting the strain-softening approach, in this study, the Mohr-Coulomb failure has been adopted as a constitutive model for soil stratum without considering strain softening. The thorough correlation of experimental and numerical results strengthened the correctness of the mentioned adopted constitutive model. Appropriately, this numerical analysis is carried out employing the Finite Element (FE) code for verification through 2-Dimensional plane strain, explicit condition, and 3-Dimensional standard stress condition. As the first series of analytical models, two-dimensional models with the same size as the prototype condition were designed for both of the (i) free-field condition and (ii) mitigation model (with foundation positioning at S/B=0 and applying the mitigated scenario). The explicit model was applied to make meshes capable of more movement without the need for re-meshing which burnish the precision of numerical analysis. Furthermore, since selecting an appropriate size of mesh (measuring 1m or less) in probable parts of soil against to fault rupture is a desideratum (Gazetas et al. 2008), after several times experimenting with various mesh sizes, the best mesh dimensions in terms of both accuracy and runtime have been picked in the current numerical study. Befittingly, a mesh dimension of 0.5 × 0.5m was chosen in the area with a risk of rupture, and the mesh sizes get larger till the greatest size became 1 × 1m at soil boundaries. The soil stratum has been modeled with an elasto-plastic constitutive model with a Mohr-Coulomb failure approach due to the relatively loose sand which was used through the experiments and structured quadrilateral continuum finite element was used to model the soil body. Soil properties similar to the ones which were used for centrifuge experiments are given in Table.3. By representing a discontinuity between two parts of the soil, the hydraulic jack-induced displacement for simulating the reverse fault was applied to the moveable part (hanging wall), and the stationary part (footwall) got deprived of any motion by applying fixed boundary conditions.

The foundation was modeled at the position of S/B=0, as a linear elastic beam element with high rigidity (steel) and the same dimensions as the prototype scale. Used to test with an aluminum plate during the centrifuge experiments, the inclined wall was modeled as a linear elastic solid element, cuboid shape with a typical density and stiffness of concrete and the same size as the prototype scale. The properties of materials of both surface foundation and the inclined wall used in the numerical simulation are depicted in Table.4. The interaction between both foundation-soil and concrete wall-soil were defined by contact type interface with the normal behavior of hard contact and friction coefficient of "μ" for tangential behavior. The probability of any separation at the contact level between every two elements among soil, foundation, and concrete wall, gap element specifications were introduced to the models; consequently, each element which is rigid in compression and tensionless was allowed for any detachment. The meshing of the inclined wall was modeled using 0.5 × 0.5 m structural quad elements. Following the designing procedures, the gravity load was applied to the whole system including soil, surface foundation, and inclined wall, as the first step of loading. Then, the right side of the soil (which represented the hanging wall) was moved upward at the dip angle of 75°, while the left side remains moveless as fixed boundary conditions were applied. The vertical boundaries were free to move in a vertical direction whilst the horizontal boundaries were completely fixed. Both the boundary conditions and meshes used in two-dimensional finite element modeling are shown in Fig.7.

Table 4. Summary of material properties using to model the surface foundation, the inclined concrete wall, and correspondingly, the row of micro-piles

Material	Unit weight (kN/m^3)	Elastic modulus (GPa)	Poisson's ratio	Friction coefficient, μ
Steel	77.142	200	0.35	0.35
Concrete	24	25	0.28	0.4

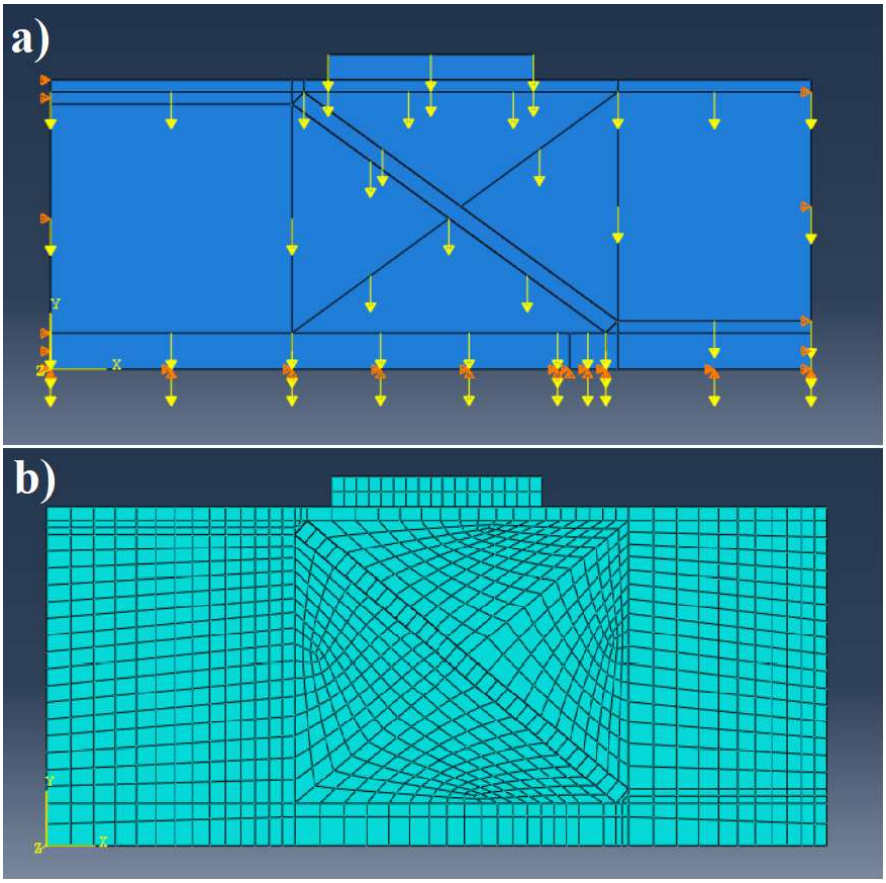

Fig.7. Two-dimensional Finite Element modeling; (a) boundary conditions, (b) meshing

Turning to the second series of numerical modeling, both the mentioned models including (i) free-field test and (ii) mitigated model were designed in three-dimensional space, as well. 3D modeling aimed to make not only a more accurate observation and better comparison between the experimental and numerical results, but also a ground for preparing an appropriate condition for following parametric investigations. 3D models were designed with the same material and interaction properties, boundary conditions, and meshing strategy with 3D stress standard FE modeling. The soil system, foundation element, and concrete slab element, all were modeled in three-dimensional condition consists of an 8-node quadratic brick. Analytical predictions are compared with centrifuge model test results in terms of: (a) vertical displacement of the surface in free-field condition; and (b) rotation of surface foundation at S/B=0 under the influence of a fault rupture of 75°. Vertical displacement of the surface during the free-field physical and numerical tests when they are subjected to a reverse fault of dip angle 75 degree occurs is predicted in Fig.8. It illustrates how an exact fit is achieved between the numerical and experimental results. Also, the exact rotation of the foundation in all numerical and physical tests are shown in Fig.9.

The numerical modeling for both 2D and 3D conditions and experimental results at h=48 mm (2.4 m at prototype scale) for free field condition were compared in (Fig.10). As it can be observed, there is a kind of affinity between the rupture paths which happened in the shear zone in numerical models (Fig.10c and e) and the one which was occurred in the experimental result during the free-field test (Fig.10a). Based on the mentioned analogy, the efficiency of the finite element method can be proven, precisely. Moreover, Fig.10b displays the results of fault rupturing of a surface foundation and an inclined wall when they subject to a reverse fault of 75-degree. Fault rupture is stimulated to propagate and deviate along the inclined wall. Both the maximum force and strain that were applied from the ground to the surface of the foundation were limited with the help of the inclined wall. As seen (Fig.10d and f), both the 2D and 3D numerical models correlate well with the experimental results, and foundation rotation in physical and numerical studies are similar. Also, 3D models illustrated more capability to follow the displacement in physical tests and their behavior is more perfectly fit to experiment results in comparison with 2D models.

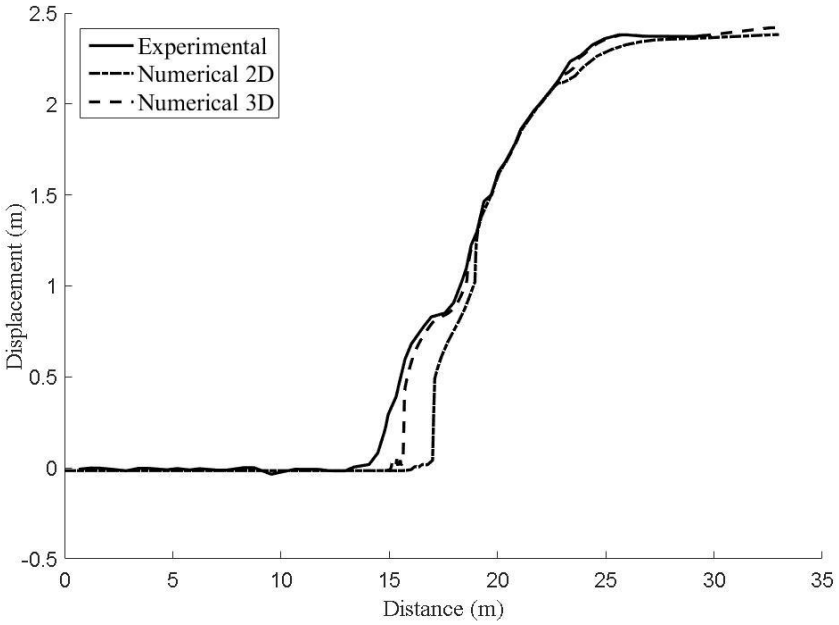

302

303 Fig. 8. Vertical displacement of the surface when the fault throw is 2.4 m, both Experimental and Numerical results

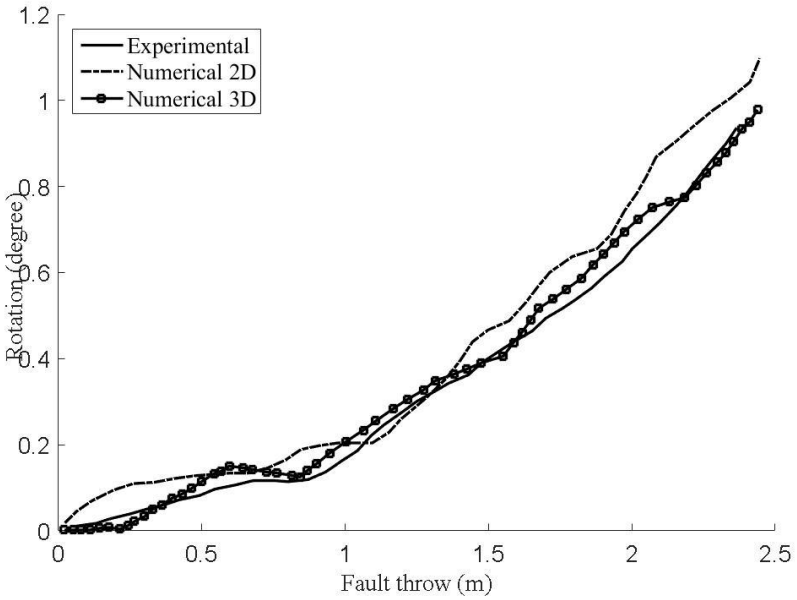

304

305 Fig. 9. Rotation of surface foundation locating at S/B=0 versus vertical throw of the fault

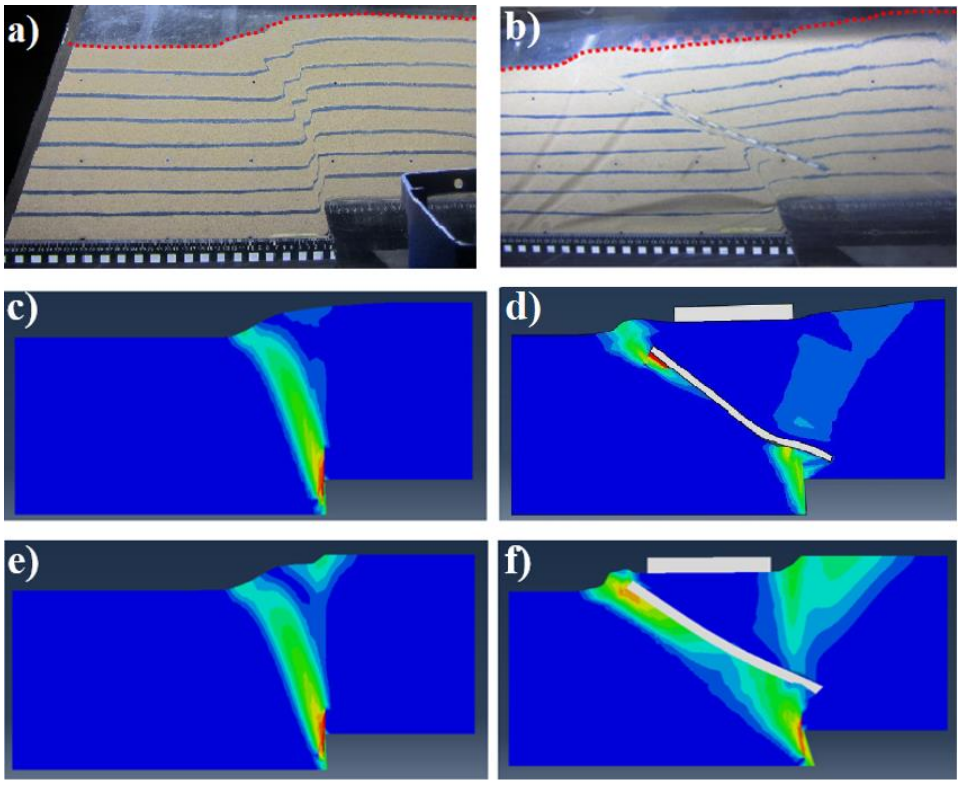

Fig. 10. Comparison between the centrifuge experiments and both 2-Dimensional and 3-Dimensional numerical analysis; (a) centrifuge model for the free-field condition; (b) centrifuge model for the test with an inclined wall when a surface foundation was positioned at S/B=0; (c) the 2-Dimensional deformed mesh with plain strain contours for the free-field condition in finite element analysis; (d) the 2-Dimensional deformed mesh with plain strain contours for the test with an inclined wall when a surface foundation was positioned at S/B-0; (e) the 3-Dimensional deformed mesh with standard 3D stress for the free-field condition; (f) the 3-Dimensional deformed mesh with standard 3D stress for the test with an inclined wall when a surface foundation was positioned at S/B=0.

Once the validation of numerical modeling was done, the verified 3D finite element model is used to investigate the efficiency of dividing the stiff inclined wall into separated inclined micro-piles. The reason behind this proposed approach is the fact that trenching a strong inclined wall (SIW) might be difficult for construction especially when it comes to the existing buildings. Therefore, to solve this complexity, it is suggested that the strong inclined wall (SIW) turns into a row of micro-piles that are installed parallel to the surface foundation. The 3D space of ABAQUS can provide us with the ability to model and evaluate elements such as micro-piles which can only be modeled in 3-Dimensional space, not in 2-Dimensional plain strain. The designing parameters of SIW were explained meticulously before. As for the designing parameters of SIMPs, all of the parameters including their length and diameter, material properties, interaction properties, and applied load were chosen similar to SIW's design parameters. In other words, micro-piles were modeled as linear elastic solid elements, with concrete properties as their material, in a linear design, just next to the surface foundation within 0.5 m of its left side. Contact interaction with the normal behavior of hard contact and isotropic tangential behavior with the friction coefficient of concrete (μ = 0.4) was adopted for the interaction of micro-piles-soil. The meshing of the inclined micro-piles was modeled using 0.5 × 0.5 m hexahedral meshes. Gravity loading, similar to what was modeled for the strong inclined wall, was first put to the whole model, including micro-piles; then, fault displacement was applied as the second step, through a dynamic explicit step, to the hanging wall.

First, to validate the process of separating the strong inclined wall (SIW) into some strongly inclined micro-piles (SIMPs), a row of circular section micro-piles with the same inclination ratio (36degree) and diameter (0.5 m) as the wall were modeled in 3D space which were completely tangent to each other. Fig.11 delineates a comparison between the stiff inclined wall and stiff inclined micro-piles in a tangential mode. As it is clear, the amount of rotation due to the fault throw factor is approximately the same in both the SIW and inclined tangential micro-piles (SIMPs).

Lastly, a series of 40 numerical analyses of 8-nodal continuum elements with various fundamental parameters of designing was investigated to observe the efficiency of conducting SIMPs besides a surface foundation locating at S/B=0 to mitigate the fault rupture of dip angle both 60degree and 75degree. Those fundamental parameters were picked as all the practical factors of conducting such micro-piles including both its structural characterization and placing parameters were considered. The effectiveness of those parameters was evaluated as the parametric study.

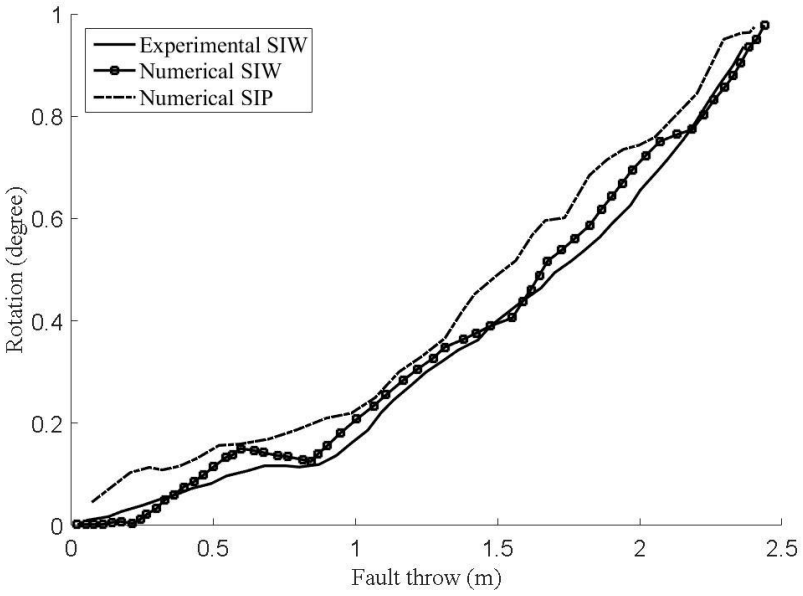

Fig. 7. Rotation of surface foundation protected by both SIW and tangential SIMPs versus vertical throw of the fault

Parametric Study

With regards to the efficiency of executing an inclined wall to mitigate the fault rupture, it has been suggested that subdividing the mentioned inclined wall into a row of micro-piles seems to be a great approach in terms of deviating fault rupture. Therefore, micro-piles divided from the inclined concrete wall were numerically investigated with the Mohr-Coulomb failure approach model in the finite element code ABAQUS software. Correspondingly, this section summarizes the result of parametric studies on the various parameters of designing a group of SIMPs which if they were modeled in a tangential outlook, a concrete inclined wall would appear, same as what was modeled in the physical and numerical tests. The efficiency of the suggested mitigation approach is a function of several parameters which the key design parameters include the diameter of micro-piles, angle of installation, and the favorable distance between every two consecutive micro-piles was studied.

Effect of Inclination

For choosing the optimum slope of micro-piles, some parametric studies were conducted considering three different amounts of angle including 20°, 30°, and 40°. To highlight the effect of inclination, the diameter of each micro-pile was 25cm and the distance between them picked as 50cm.

Choosing the appropriate slope for the SIMPs is of that important, since having 20-degree of inclination led to a little higher foundation rotation compared with unprotected when the fault throw is fewer than an approximate amount of 0.35 m. As seen, increasing micro-piles' slope results in better performance in terms of diverting the fault rupture; consequently, micro-piles with inclination amounts 40degree effectively reduced damage to a negligible amount (Fig.12).

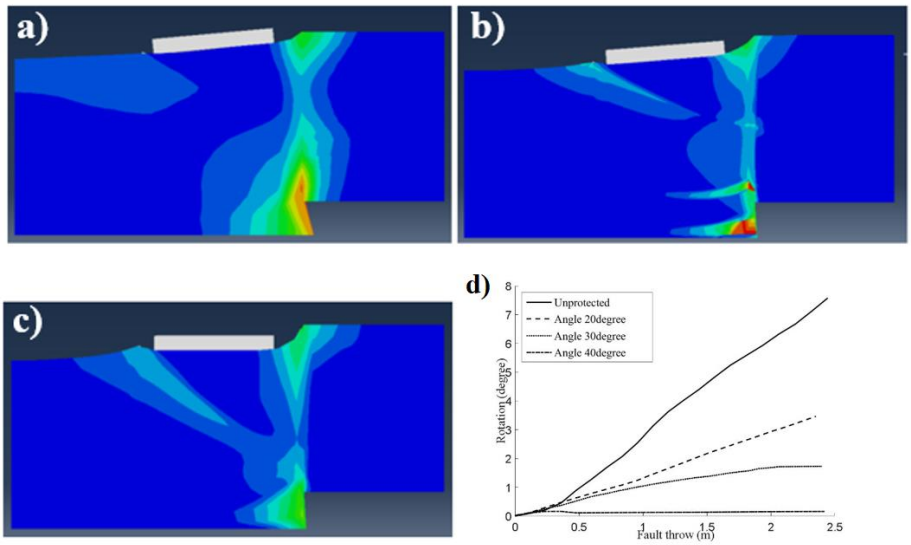

Fig. 8. The effect of inclination on micro-piles; (a) inclined micro-piles of 20-degree; (b) inclined micro-piles of 30-degree; (c) inclined micro-piles on 40-degree; (d) the amount of rotation of the protected surface foundation

Effect of Diameter

Focusing on the effect of diameter, we compared the response of a row of SIMPs when they implement with an angle of 40° and the distance between every two centers of the micro-piles was 50 cm against a reverse fault rupture. To consider the effect of diameter, three different amounts of diameters including 10, 20, and 25 centimeters as the diameter of each micro-pile that were installed in a linear row were picked and investigated. As can be seen, Fig.13 depicts that the more the diameter becomes, the fewer the shallow foundation rotates. Also, applying SIMPs of any diameter can reduce fault rupture to a significant amount except micro-piles with 10cm diameter and inclination of 20degree. Despite the efficiency of conducting such micro-piles with any diameter, it is obvious that the most satisfactory result can be achieved from implementing SIMPs with a diameter of 25cm and an inclination angle of 40degree. For the mentioned parameters, the surface foundation which was located beside a row of micro-piles with a distance of 50cm between every two consecutive micro-piles, experienced about 10 times fewer rotation when the diameter of micro-piles became 25cm from 10cm.

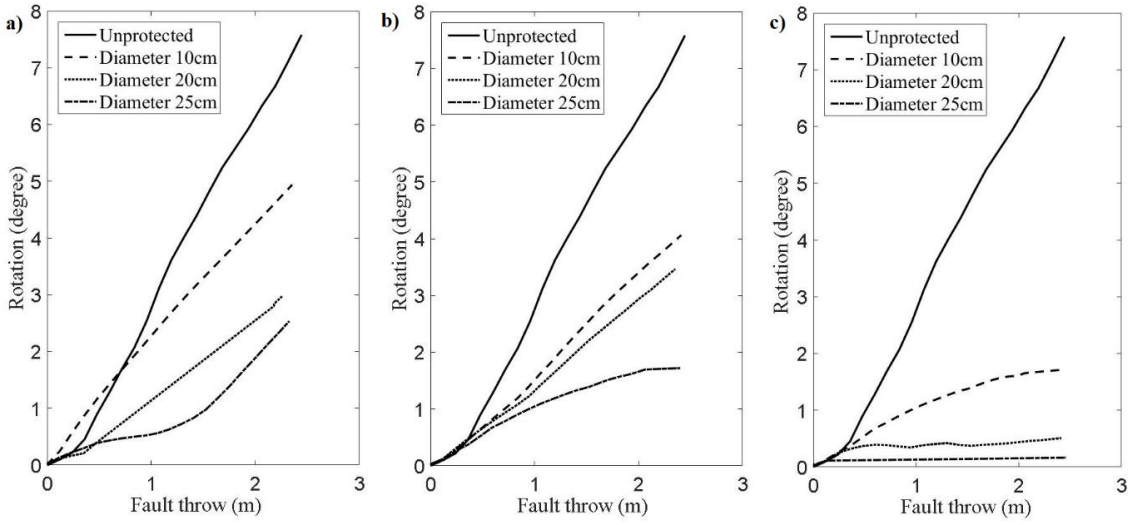

Fig.13. The effect of diameter on SIMPs when they are located with 50cm placing between every two consecutive micro-piles; (a) inclination angle of 20degree; (b) inclination angle of 30degree; (c) inclination angle of 40degree.

Effect of Distance

The last parameter in implementing SIMPs is selecting an appropriate distance between each micro-pile. The "distance" refers to the amount of space between two centers of two consecutive micro-piles locating next to each other in the row. The parametric study was carried out by making other parameters fixed including a fixed amount of 25cm for the diameter of micro-piles and 40° for the inclination of placing micro-piles into the soil. Two different amounts were given as the distance between micro-piles: 50 and 75cm. As it is illustrated in Fig.14, as the distance between micro-piles in a row increases, the shallow foundation rotates to a great degree. Furthermore, it should be mentioned that conducting SIMPs with spacing amounts of 75cm between every two consecutive micro-piles leads to more rotation compared to the unprotected condition when the fault throw is fewer than an approximate amount of 1m, 0.4m, and 0.3m for installation angle of 20degree, 30degree, and 40degree, respectively.

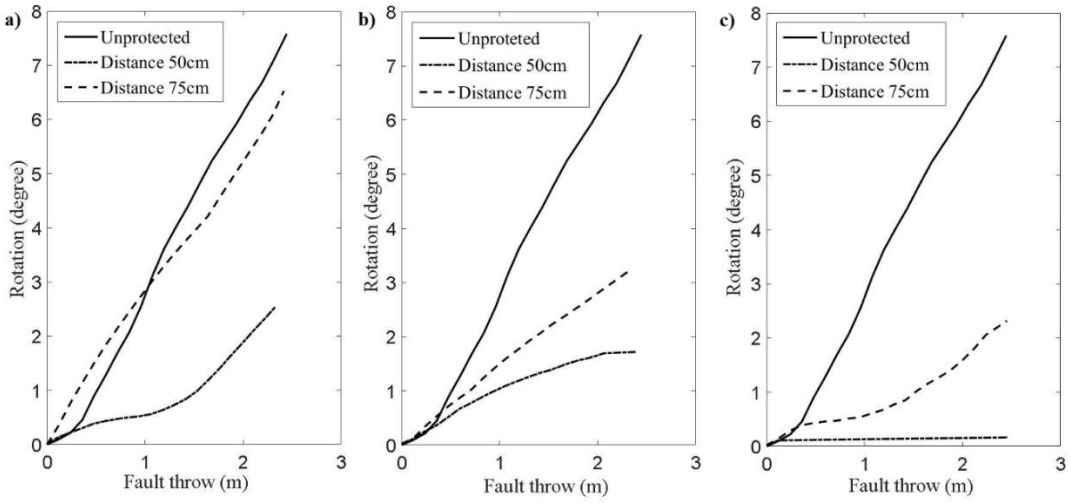

Fig.14. surface foundation rotation versus fault throw, when the foundation is protected by SIMPs with installation angle of (a) 20degree, (b) 30degree, (c) 40degree

Effect of Dip Angle

With regards to all three mentioned parameters in both designing and conducting SIMPs, the summary of how a surface foundation exhibits response when it is positioned at the free-field condition and at the same time, is protected by strongly inclined micro-piles is represented in Table.5 and 6. As is illustrated, implementing SIMPs with a diameter amount of either 20 or 25cm, spacing content of 50cm, and installation angle of 40degree can enhance the surface foundation rotation from about 8degree when it is not protected to a negligible amount of fewer than 1degree against fault rupture of dip angle 75degree. It can be seen that finding appropriate designing parameters for SIMPs should be considered as a key factor since it can enhance the status of foundation rotation from severe into a reassuring one with just a negligible amount of rotation. Furthermore, Table.5 shows that to mitigate the fault rupture of dip angle 60degree, conducting SIMPs with a diameter of either 20 or 25cm, an installation angle of both 30degree and 40degree, and spacing amount of 50cm can lead the surface foundation to a rotation fewer than 2degree. Also, it is noticeable that the most favorable result can be gained through conducting SIMPs with a diameter of 25cm and installation angle of 30degree with a spacing of 50cm between each micro-pile which can reduce the rotation of surface foundation from more than 12degree to about 1.5degree.

410 Table 5. Summary how each factor of SIMPs affects the surface foundation rotation (75degree of dip angle)

0≤Rotation(θ) <1°	1°≤Rotation(θ) <2°	2°≤Rotation(θ) <5°	5°≤Rotation(θ) °
Negligible to slight	Slight to moderate	Severe	Threatening stability
The angle of installation 20degree			
Distance / Diameter	d = 10 cm	d = 20 cm	d = 25 cm
h_s = 50 cm			
h_s = 75 cm			
The angle of installation 30degree			
Distance / Diameter	d = 10 cm	d = 20 cm	d = 25 cm
h_s = 50 cm			
h_s = 75 cm			
The angle of installation 40degree			
Distance / Diameter	d = 10 cm	d = 20 cm	d = 25 cm
h_s = 50 cm			
h_s = 75 cm			

411

412 Table 6. Summary of how each factor of SIMPs affects the surface foundation rotation (60degree of dip angle)

0≤Rotation(θ) <1°	1°≤Rotation(θ) <2°	2°≤Rotation(θ) <5	5°≤Rotation(θ) °
Negligible to slight	Slight to moderate	Severe	Threatening stability
The angle of installation 20degree			
Distance / Diameter	d = 10 cm	d = 20 cm	d = 25 cm
h_s = 50 cm			
h_s = 75 cm			
The angle of installation 30degree			
Distance / Diameter	d = 10 cm	d = 20 cm	d = 25 cm
h_s = 50 cm			
h_s = 75 cm			
The angle of installation 40degree			
Distance / Diameter	d = 10 cm	d = 20 cm	d = 25 cm
h_s = 50 cm			
h_s = 75 cm			

Critical Positions of Surface Foundation

Since there remain some critical positions (S/B= -0.25, 0, and 0.25) in protecting a surface foundation using a Weak Vertical Wall (WVW) (Baziar et al., 2019), these positions were chosen to investigate the efficiency of mitigating fault rupture by conducting a row of SIMPs. Results of both protected by either SIMPs or a WVW and unprotected surface foundation rotations when the foundation is positioned at mentioned critical locations subjecting to reverse fault of dip angle 60-degree and 75-degree are illustrated in Fig.15 and 16. As is illustrated, conducting SIMPs with proper designing factors results in enhancing the surface foundation's rotation when a WVW cannot mitigate the fault rupture hazards. The comparison between both reverse faults shows that increasing fault dip angle leads to larger rotations.

For reverse fault rupture of dip angle 60degree, S/B=0 is the worst position in terms of rotating the surface foundation. It can be observed that conducting a row of SIMPs with appropriate features (diameter of 25cm, a distance of 50cm between every two consecutive micro-piles, and 40degree as the angle of installation) for S/B=0 can enhance the rotation of surface fault from an extreme amount ($\theta>12^{\circ}$) to a moderate level ($\theta<2^{\circ}$) and hence, reduce the damage level. Also, it is obvious that the closer the surface foundation gets to the hanging wall (S/B=-0.25), the less the efficiency of micro-piles is. However, even for S/B=-0.5, conducting SIMPs can reduce the amount of rotation of the surface foundation to its third in comparison with the unprotected situation (Fig.15 a)

Turning to reverse fault rupture of dip angle 75degree (Fig.15 b), the surface foundation at S/B=+0.25 experiences the highest rotation ($\theta>12^{\circ}$). Implementing a row of SIMPs with previously applied features (diameter of 25cm, a distance of 50cm between every two consecutive micro-piles, and 40degree as the angle of installation) can improve this extreme rate of rotation to a slight level ($\theta\leq1^{\circ}$). Also, the highest efficiency of conducting stiff inclined micro-piles can be found when the surface foundation is positioned at the free-field condition. Conducting such micro-piles when the surface foundation is placed at S/B=0 can ameliorate the surface foundation's rotation from a threatening level ($\theta>8^{\circ}$) to a negligible amount ($\theta<0.5^{\circ}$). Nevertheless, the effectiveness of conducting SIMPs gets less as the surface foundation becomes closer to the fault rupture and for the position of S/B=0.25, conducting stiff inclined micro-piles seems to do nothing to mitigate the fault rupture.

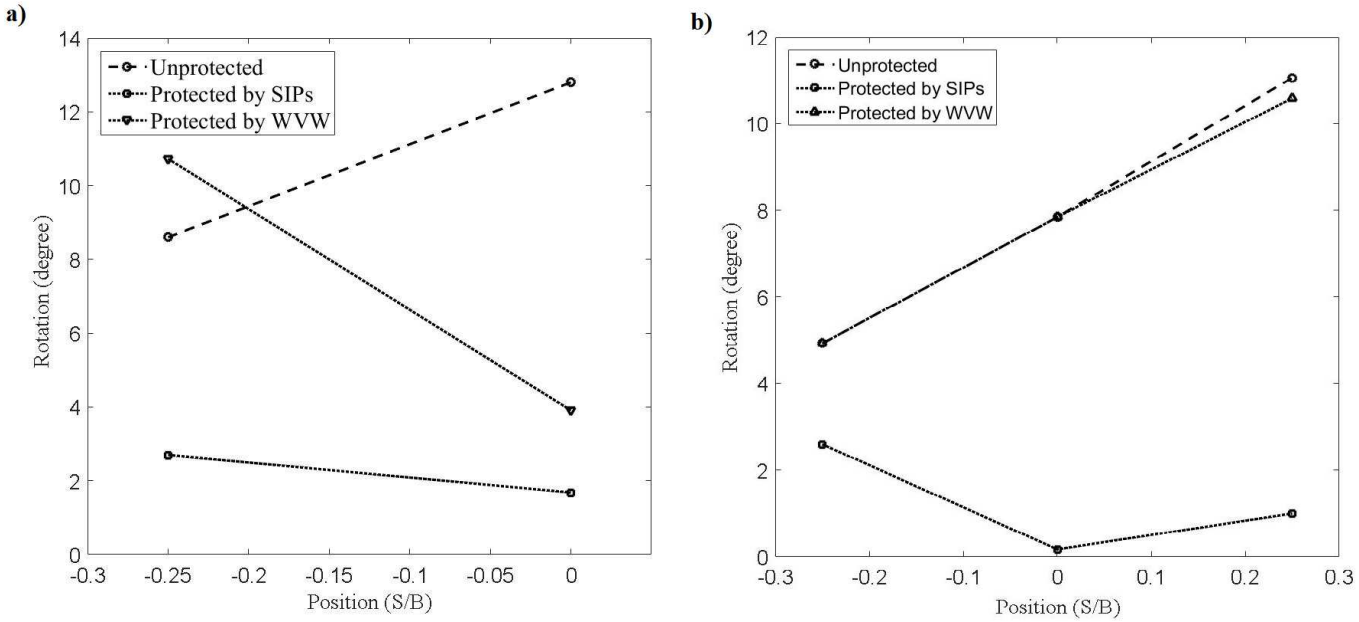

Fig. 15. Effectiveness of conducting either SIMPs or a Weak Vertical Wall (WVW) to protect surface foundation against fault rupture of dip angle (a) 60degree, (b) 75degree.

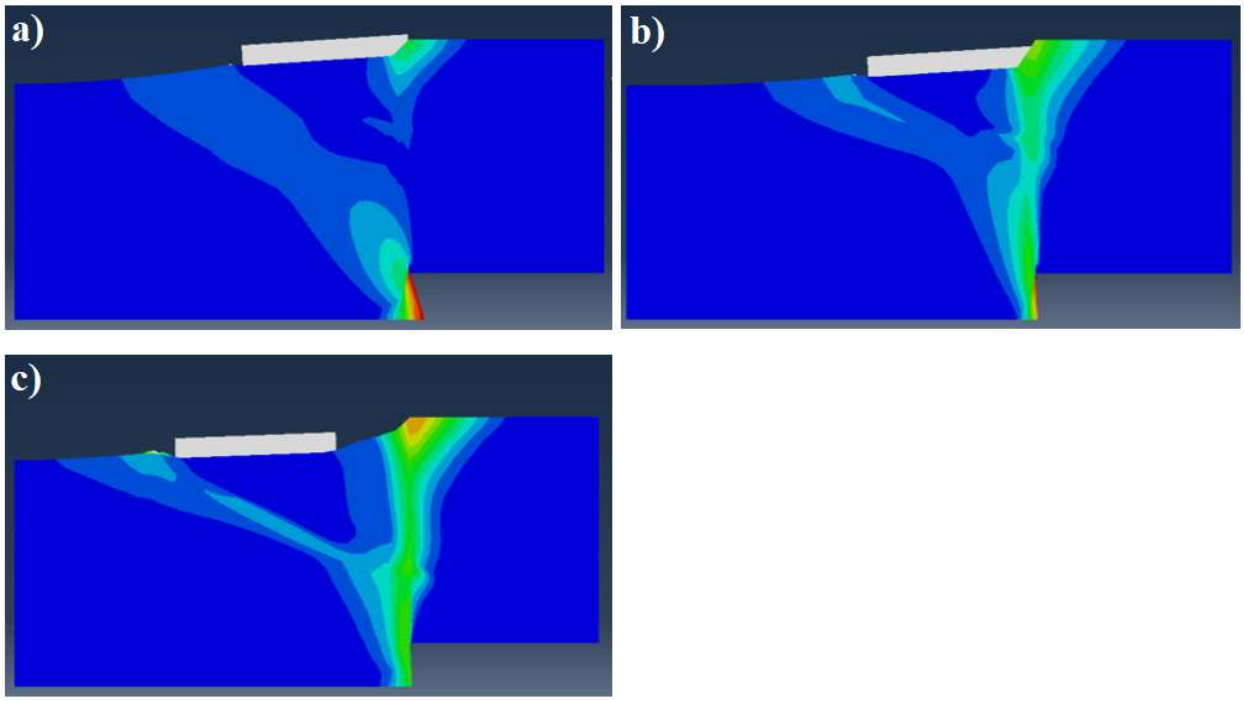

Fig. 16. Numerical results of how a row of SIMPs affect the rotation of a surface foundation which is placed at (a) S/B=-0.25 against fault rupture of dip angle 60degree, (b) S/B=-0.25 against fault rupture of dip angle 75degree, (c) S/B=+0.25 against fault rupture of dip angle 75degree.

Conclusion

In this research, we analyzed the efficiency of applying a strong inclined wall (SIW) to protect surface foundations against reverse fault ruptures of dip angle 75degree investigated both physically and 3-Dimensional numerically as well as 2-Dimensional. As seen, results have shown that 3-Dimensional modeling provides a better degree of accuracy with regard to the centrifuge experiments than the 2-Dimensional models. Afterward, the effectiveness of subdividing the SIW into some separated strong inclined micro-piles (SIMPs) with the same material properties numerically examined. Consequently, based on numerical analysis using the finite element analysis, the following conclusions can be drawn from the research:

1. While placing a weak vertical element cannot protect the surface foundation against rotating throughout fault rupture of dip angle 75degree, trenching a strong inclined wall (SIW) which has a greater shear strength compared to its surrounding soil, beneath the surface foundation, can deviate fault rupture path and reduce the amounts of foundation rotation. In other words, SIW can reduce the surface foundation's rotation to lower degrees to acceptable values. For this specific purpose, the strong inclined wall should possess an appropriate thickness (0.5 m for the presented case). However, it should be mentioned that there are some limitations for SIW, including the maximum force and strain applied from the ground to the foundation.
2. The strongly inclined micro-piles (SIMPs) which can be subdivided from SIW are considered as a more convenient approach to solve the complication of placing SIW for existing structures. A row of SIMPs with a circular section area which is placed in a tangential outline, with the same shear strength as the SIW, can reduce the foundation rotation approximately the same as how much the SIW can mitigate.
3. The diameter of SIMPs and their installation angle play a crucial role in mitigating fault rupture. While SIMPs with a diameter of 10cm with an installation angle of 20degree lead to more rotation of foundation compared to unprotected condition, SIMPs with a 25cm diameter and installation angle of 40degree result in a negligible amount of foundation rotation ($\theta<0.5^{\circ}$).
4. The spacing amount between every two consecutive micro-piles is another significant factor to mitigate fault rupture. Increasing the mentioned distance can reduce the efficiency of SIMPs. A distance of 50 centimeters can be considered as a satisfactory amount to reduce foundation rotation.

5. Using the novel approach of placing SIMPs can also reduce the rotation of surface foundation which are placed at other critical positions that cannot be mitigated with the help of a weak vertical wall including S/B=-0.25 and +0.25 were investigated. For the fault rupture of dip angle 75degree, the amount of rotation of surface foundation at S/B=+0.25 dropped to a moderate amount from a threatening situation while, conducting such SIMPs besides a surface foundation which is located at S/B=-0.25 seems to have no considerable effect. Also, for the fault rupture of dip angle 60degree, implementing SIMPs can mitigate the surface foundation placing at S/B=-0.25 and reduce rotation to about a quarter of the amount of rotation when it is unprotected.

The finding of this research presents that conducting a weak vertical wall (WVW) and a row of strongly inclined micro-piles (SIMPs) simultaneously, results in protecting a surface foundation against fault rupture of dip angle 60 and 75degree. However, it should be mentioned that the effectiveness of the SIMPs depends mainly on the fault dip angle, the diameter of micro-piles, the distance between every two consecutive micro-piles, and their installation angle. The ideal combination of all mentioned parameters according to the soil properties, foundation location, and surcharge load for the existing structures can result in mitigating the fault rupture

Data Availability Statement

Some or all data and models that support the finding of this research are available from the corresponding author upon request.

Funding Source Declaration

This research received no specific grant from any funding agency in the public, commercial, or not-for-profit sectors.

Notation

The following symbols are used in this paper:

B = foundation's breadth;

D_{50} = a cumulative 50% point of diameter;

d = distance between each two consecutive micro-piles;

e_{max} = void ratio of coarse-grained soil (cohesionless) in its loosest state;

e_{min} = void ratio of coarse-grained soil (cohesionless) in its densest state;

g = acceleration due to gravity;

H = soil thickness;

h = vertical throw;

h_s = micro-pile's diameter;

M_w = moment magnitude scale of an earthquake;

q = foundation's surcharge load;

S = relative situation of the foundation toward the fault rupture;

α = fault dip angle;

β = angle of installation of strong inclined wall (SIW);

θ = foundation's rotation;

ϕ_p = peak friction angle of soil;

$\phi_{residual}$ = residual friction angle of soil;

Ψ_p = peak dilation angle of soil;

γ_{wet} = soil unit weight;

References

Abdoun, T., Dobry, R., O'Rourke, T. D., & Goh, S. H. (2003). Pile response to lateral spreads: centrifuge modeling. Journal of Geotechnical and Geoenvironmental Engineering, 129(10), 869-878. https://doi.org/10.1061/(ASCE)1090-0241(2003)129:10(869)

Anastasopoulos, I., et al. 2007. "Fault rupture propagation through sand: finite-element analysis and validation through centrifuge experiments." Journal of geotechnical and geoenvironmental engineering 133(8): 943-958. https://doi.org/10.1061/(ASCE)1090-0241(2007)133:8(943)

Anastasopoulos, I. & Gazetas, G. 2007. "Foundation–structure systems over a rupturing normal fault: Part I. Observations after the Kocaeli 1999 earthquake." Bulletin of Earthquake Engineering, 5, 253-275. https://doi.org/10.1007/s10518-007-9029-2

Anastasopoulos, I. & Gazetas, G. 2007. "Foundation–structure systems over a rupturing normal fault: Part II. Analysis of the Kocaeli case histories. Bulletin of Earthquake Engineering" 5, 277-301. https://doi.org/10.1007/s10518-007-9030-9

Anastasopoulos, I., Callerio, A., Bransby, M. F., Davies, M. C. R., Nahas, A. E., Faccioli, E., Gazetas, G., Masella, A., Paolucci, R., Pecker, A. & Rossignol, E. 2008. "Numerical analyses of fault–foundation interaction." Bulletin of Earthquake Engineering, 6, 645-675. https://doi.org/10.1007/s10518-008-9081-6

Anastasopoulos, I., Gazetas, G., Bransby, M. F., Davies, M. C., & El Nahas, A. 2009. "Normal fault rupture interaction with strip foundations." Journal of Geotechnical and Geoenvironmental Engineering, 135(3), 359-370. https://doi.org/10.1061/(ASCE)1090-0241(2009)135:3(359)

Anastasopoulos, I., Antonakos, G. & Gazetas, G. 2010. "Slab foundation subjected to thrust faulting in dry sand: Parametric analysis and simplified design method." Soil Dynamics and Earthquake Engineering, 30, 912-924. https://doi.org/10.1016/j.soildyn.2010.04.002

Ashtiani, Mehdi, Abbas Ghalandarzadeh, and Ikuo Towhata. 2015. "Centrifuge modeling of shallow embedded foundations subjected to reverse fault rupture." Canadian Geotechnical Journal 53.3: 505-519. https://doi.org/10.1139/cgj-2014-0444

Ashtiani, M., Ghalandarzadeh, A., & Towhata, I. (2016). Centrifuge modeling of shallow embedded foundations subjected to reverse fault rupture. Canadian Geotechnical Journal, 53(3), 505-519.https://doi.org/10.1139/cgj 507-2014-0444

Ashtiani, M., et al. 2017. "Centrifuge modeling of geotechnical mitigation measures for shallow foundations subjected to reverse faulting." Canadian Geotechnical Journal (ja). https://doi.org/10.1139/cgj-2017-0093

Azizkandi, A. S., Ghavami, S., Baziar, M. H., & Hasanaklou, S. H. (2019). Assessment of damages in fault rupture–shallow foundation interaction due to the existence of underground structures. Tunneling and Underground Space Technology, 89, 222-23. https://doi.org/10.1016/j.tust.2019.04.005

Baziar, M.H., Nabizadeh, A., Jabbari, M., 2012. "Evaluation of fault–foundation interaction using numerical studies." In: 15th world conference on earthquake engineering. Lisbon, Portugal, 24–28 September 2012

Baziar, M. H., Hasanaklou, S. H., & Azizkandi, A. S. 2019. "Evaluation of EPS wall effectiveness to mitigate shallow foundation deformation induced by reverse faulting." Bulletin of Earthquake Engineering, 17(6), 3095-3117. https://doi.org/10.1007/s10518-019-00581-9

Baziar, M. H., Nabizadeh, A., Khalafian, N., Lee, C. J., & Hung, W. Y. (2020). Evaluation of reverse faulting effects on the mechanical response of tunnel lining using centrifuge tests and numerical analysis. Géotechnique, 70(6), 490-502. https://doi.org/10.1680/jgeot.18.P.019

Bransby, M. F., M. C. R. Davies, and A. El Nahas. 2008. "Centrifuge modelling of normal fault–foundation interaction." Bulletin of Earthquake Engineering 6.4: 585-605.https://doi.org/10.1007/s10518-008-9079-0

Bransby, M. F., Davies, M. C. R., El Nahas, A., & Nagaoka, S. 2008. "Centrifuge modelling of reverse fault–foundation interaction." Bulletin of Earthquake Engineering, 6(4), 607-628.https://doi.org/10.1007/s10518-008-9080-7

Bray, Jonathan D. "The effects of tectonic movements on stresses and deformations in earth embankments". (1991). Ph.D. dissertation, Univ. of California at Berkeley, Berkeley, Calif.

Bray, Jonathan D. 2001. "Developing mitigation measures for the hazards associated with earthquake surface fault rupture." Workshop on seismic fault-induced failures—possible remedies for damage to urban facilities. University of Tokyo Press.

Bray, J. D., Seed, R. B., Cluff, L. S., & Seed, H. B. (1994). Earthquake fault rupture propagation through soil. Journal of Geotechnical Engineering, 120(3), 543-561. https://doi.org/10.1061/(ASCE)0733-9410(1994)120:3(543)

Bray, J. D., Seed, R. B., and Seed, H. B. (1994b). "Analysis of earthquake fault rupture propagation through cohesive soil." J. Geotech. Engrg., 120(3), 562–580. https://doi.org/10.1061/(ASCE)0733-9410(1994)120:3(562)

Chang YY, Lee CJ, HuangWC, HuangWJ, LinML, HungWY, Lin YH. 2013. "Use of centrifuge experiments and discrete element analysis to model the reverse fault slip." Int J Civ Eng 11(2):79–89

Choo, Y. W., Kim, D. S., Kim, K. H., Shin, D. H., Im, E. S., Cho, S. E., & Park, H. G. (2010). Effect of drainage zoning and deeply placed plinth on CFGD. In Physical Modelling in Geotechnics, Two Volume Set (pp. 1201-1206). CRC Press.

Erickson, S. G., Strayer, L. M., & Suppe, J. (2001). Initiation and reactivation of faults during movement over a thrust-fault ramp: numerical mechanical models. Journal of Structural Geology, 23(1), 11-23. https://doi.org/10.1016/S0191-8141(00)00074-2

Faccioli E, Anastasopoulos I, Gazetas G, Callerio A, Paolucci R. 2008. "Fault rupture-foundation interaction: selected case histories." Bull Earthq Eng 6(4):557–583https://doi.org/10.1007/s10518-008-9089-y

Fadaee M, Anastasopoulos I, Gazetas G, Jafari MK, Kamalian M. 2013. "Soil bentonite wall protects foundation from thrust faulting: analyses and experiment." J Earthq EngEngVib; 12(3):473–86.https://doi.org/10.1007/s11803-013-0187-8

Fadaee, M., Ezzatyazdi, P., Anastasopoulos, I., & Gazetas, G. 2016. "Mitigation of reverse faulting deformation using a soil bentonite wall: Dimensional analysis, parametric study, design implications." Soil Dynamics and Earthquake Engineering, 89, 248-261. https://doi.org/10.1016/j.soildyn.2016.04.007

Gazetas G, Pecker A, Faccioli E, Paolucci R, Anastasopoulos I. 2008. "Preliminary design recommendations for dip-slip fault–foundation interaction." Bull Earthq Eng; 6 (4):677–87. https://doi.org/10.1007/s10518-008-9082-5

Hayward, T., Lees, A. S., Powrie, W., Richards, D. J., & Smethurst, J. (2000). Centrifuge modelling of a cutting slope stabilized by discrete piles.

Kelson, K. I., Kang, K.-H., Page, W. D., Lee, C.-T. & Cluff, L. S. 2001. "Representative styles of deformation along the Chelungpu fault from the 1999 Chi-Chi (Taiwan) earthquake: geomorphic characteristics and responses of man-made structures." Bulletin of the Seismological Society of America, 91, 930-952. https://doi.org/10.1785/0120000741

Knappett, J. A., & Madabhushi, S. P. G. (2009). Influence of axial load on lateral pile response in liquefiable soils. Part I: physical modelling. Geotechnique, 59(7), 571-581. https://doi.org/10.1680/geot.8.009.3749.

Lee JW, Hamada M. 2005. "An experimental study on earthquake fault rupture propagation through a sandy soil deposit." Struct Eng/EarthqEng; 22 (1):1–13. https://doi.org/10.2208/jsceseee.22.1s

Lin ML, Chung CF, Jeng FS. 2006. "Deformation of overburden soil induced by Thrust fault slip." Eng Geol 88(1–2):70–89 https://doi.org/10.1016/j.enggeo.2006.08.004

Loukidis D, Bouckovalas G. 2001. "Numerical simulation of active fault rupture propagation through dry soil." In: Prakash S, (ed) Proceedings of the fourth international conference on recent advances in geotechnical earthquake engineering and soil dynamics, San Diego, California University of Missouri-Rolla; CDROM, paper no. 3.04

Loukidis, D. (1999). Active fault propagation through soil. Diploma Thesis, School of Civil Engineering, National Technical University, Athens.

Nakai, T., Wood, D. M., & Stone, K. J. (1995). Numerical calculations of soil response over a displacing basement. Soils and foundations, 35(2), 25-35. https://doi.org/10.3208/sandf1972.35.2_25

Oettle, N. K. & Bray, J. D. 2013a. "Fault Rupture Propagation through Previously Ruptured Soil." Journal of Geotechnical and Geoenvironmental Engineering, 139, 1637-1647. https://doi.org/10.1061/(ASCE)GT.1943-5606.0000919

Oettle, N. K. & Bray, J. D. 2013b. "Geotechnical mitigation strategies for earthquake surface fault rupture." Journal of Geotechnical and Geoenvironmental Engineering, 139, 1864-1874.https://doi.org/10.1061/(ASCE)GT.1943-5606.0000933

Paolucci, R., & Yilmaz, M. T. (2008). Simplified theoretical approaches to earthquake fault rupture–shallow foundation interaction. Bulletin of Earthquake Engineering, 6(4), 629-644. https://doi.org/10.1007/s10518-008-9081-6

White, D. J.,W. A. Take, and M. D. Bolton. (2003). "Soil deformation measurement using particle image velocimetry (PIV) and photogrammetry." 604 Géotechnique 53 (7): 619–631. https://doi.org/10.1680/geot.2003.53 605 .7.619. 606.

White, R. J., Stone, K. J. L., & Jewell, R. J. (1994). Effect of particle size on localization development in model tests on sand. In International conference centrifuge 94 (pp. 817-822).

Yilmaz MT, Paolucci R. 2007. "Earthquake fault rupture-shallow foundation interaction in undrained soils: a simplified analytical approach." Earthq Eng Struct Dyn 36(1):101–118 https://doi.org/10.1002/eqe.625

Zeping, X., Yujing, H., & Jianhui, L. (2014). Three-dimensional centrifuge modeling test of high CFRD in a narrow valley. In Vol. 2 of Proc., 8th Int. Conf. on Physical Modelling in Geotechnics (pp. 899-902).

Figures

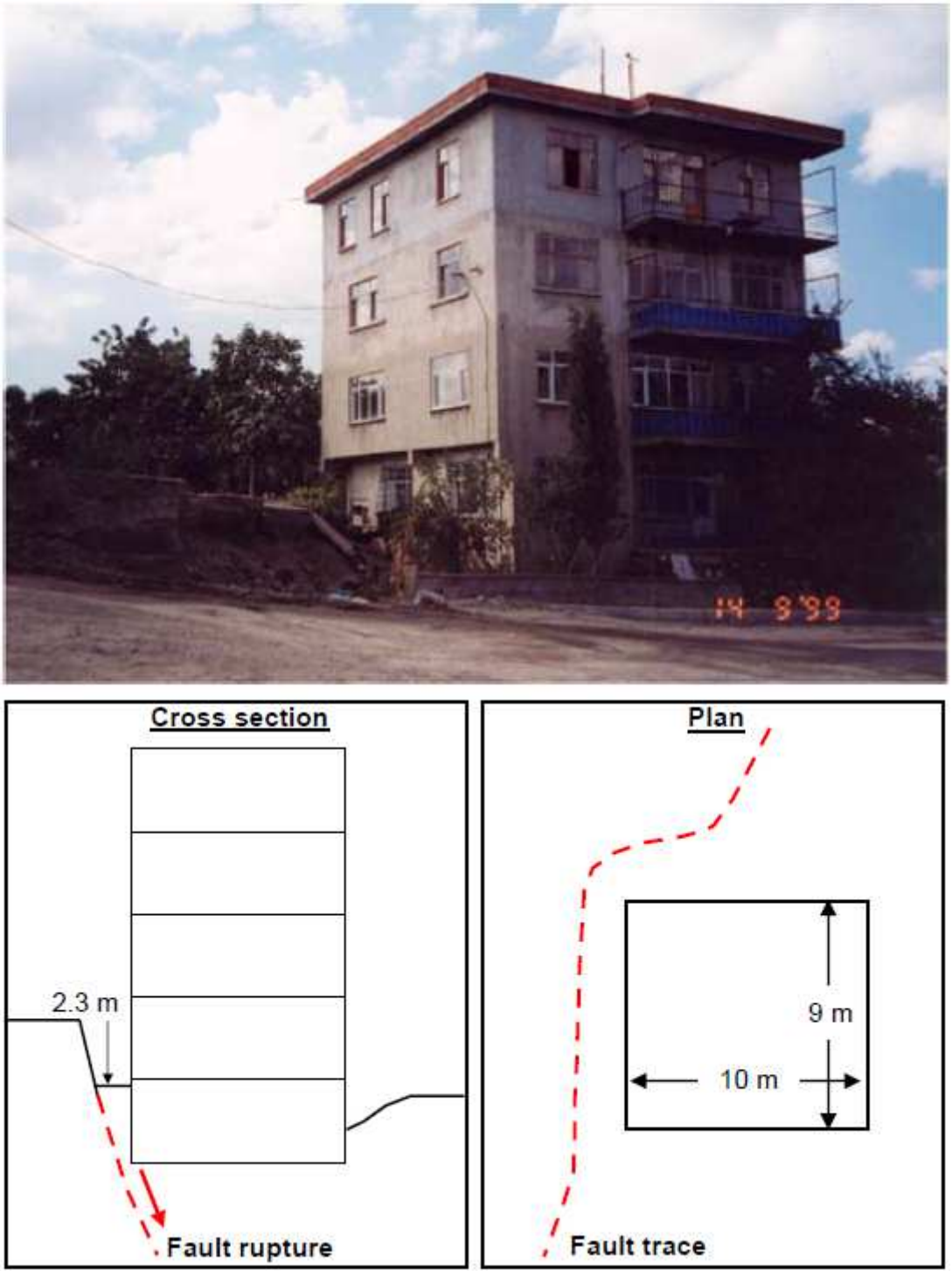

Figure 1

Normal fault east of Golcuk, Kocaeli, Turkey 1999 earthquake – Denizevler: 4-storey building with basement resting on the continuous and rigid box-type foundation. (Faccioli et al. 2008)

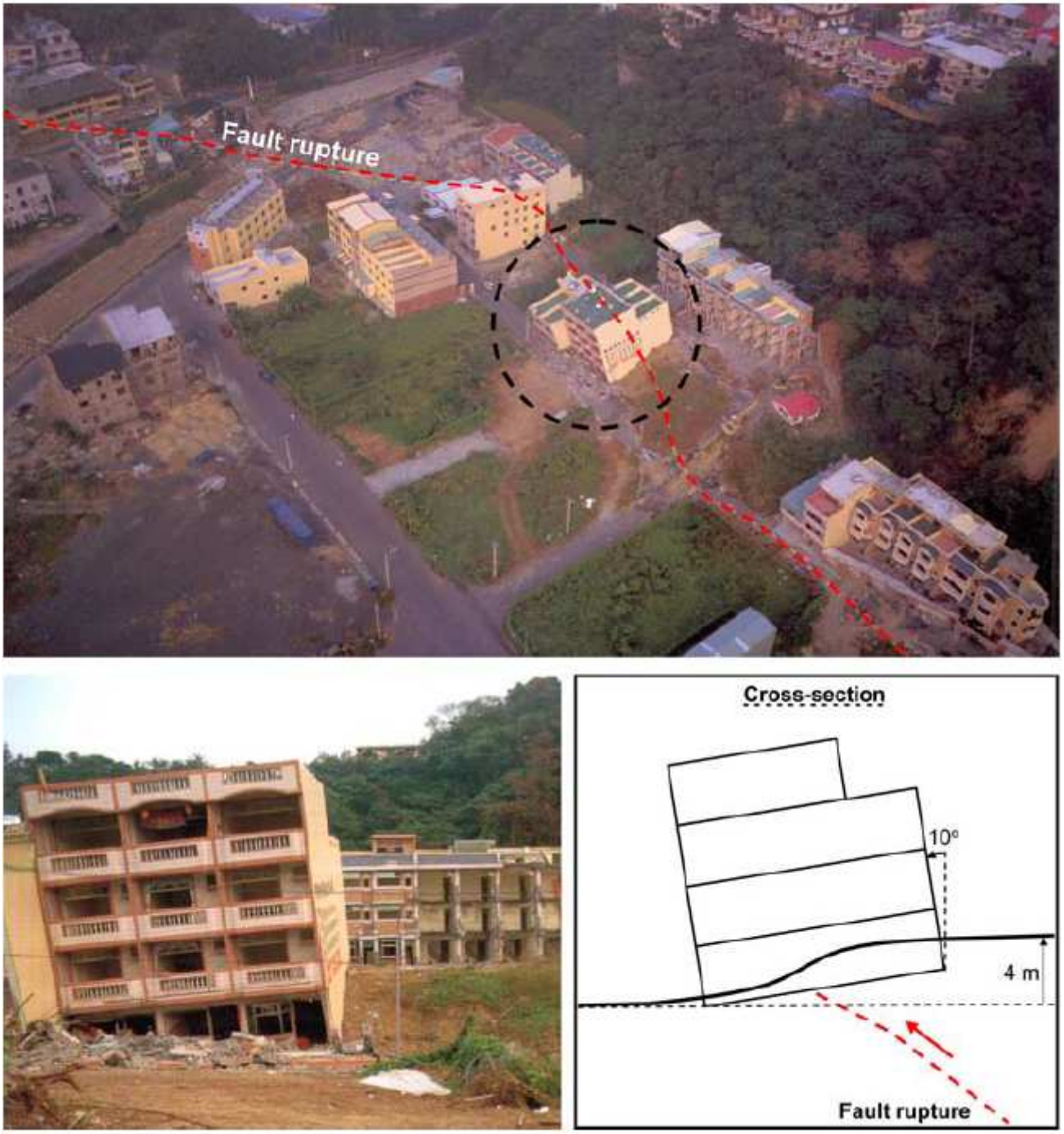

Figure 2

Chelungpu thrust fault Chi-Chi, Taiwan 1999 earthquake – Chung-Cheng Park, Fung-Yan city: 4-storey building resting on a continuous and rigid foundation (photos adopted from Hwang 2000) (Faccioli et al. 2008)

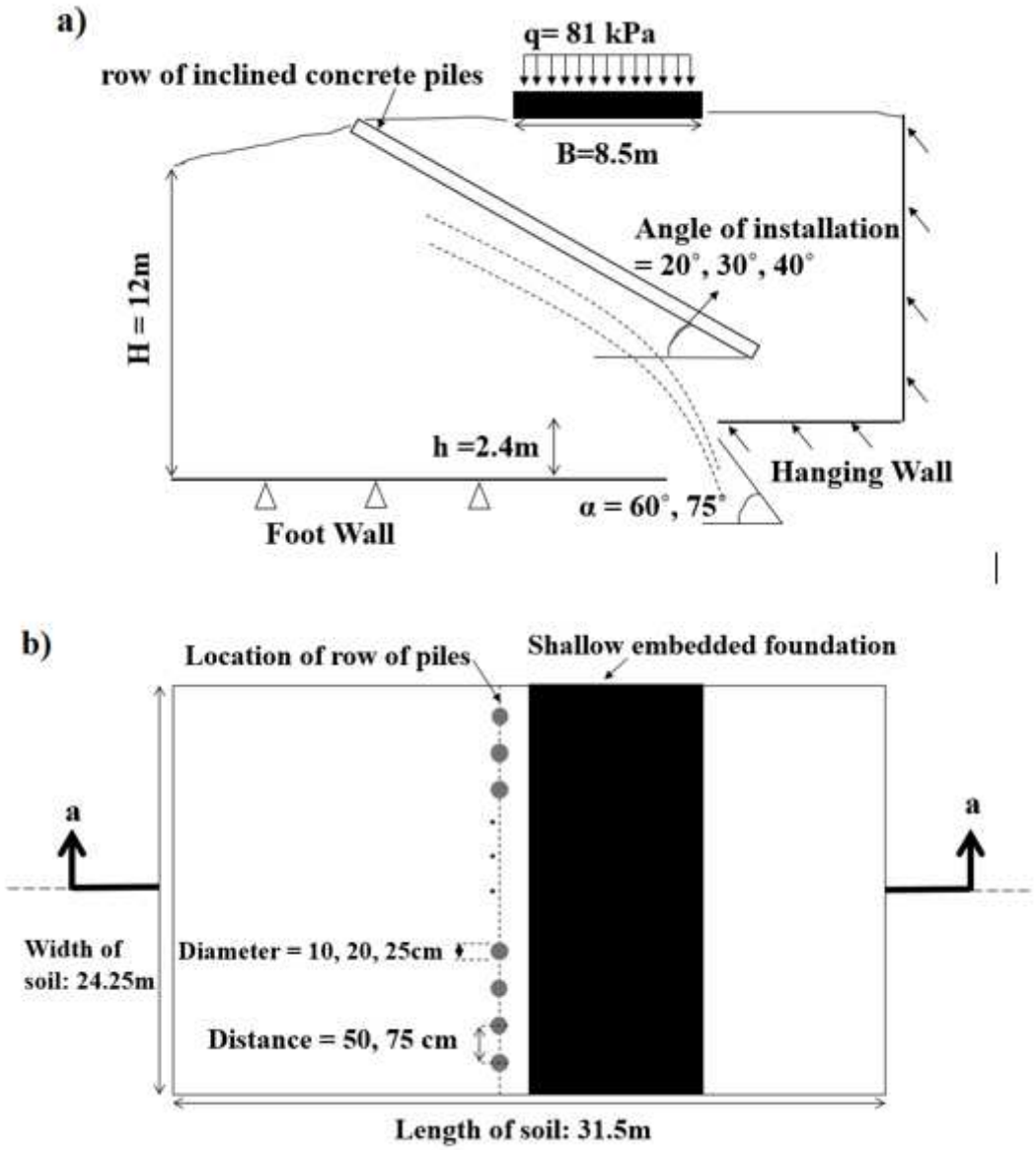

Figure 3

Schematic representation of the investigated problem; (a) the row of micro-piles suggested subdividing from the inclined concrete wall, (b) cross-section a-a of the 3D finite element discretization, showing the place of micro-piles and the parameters which were investigated.

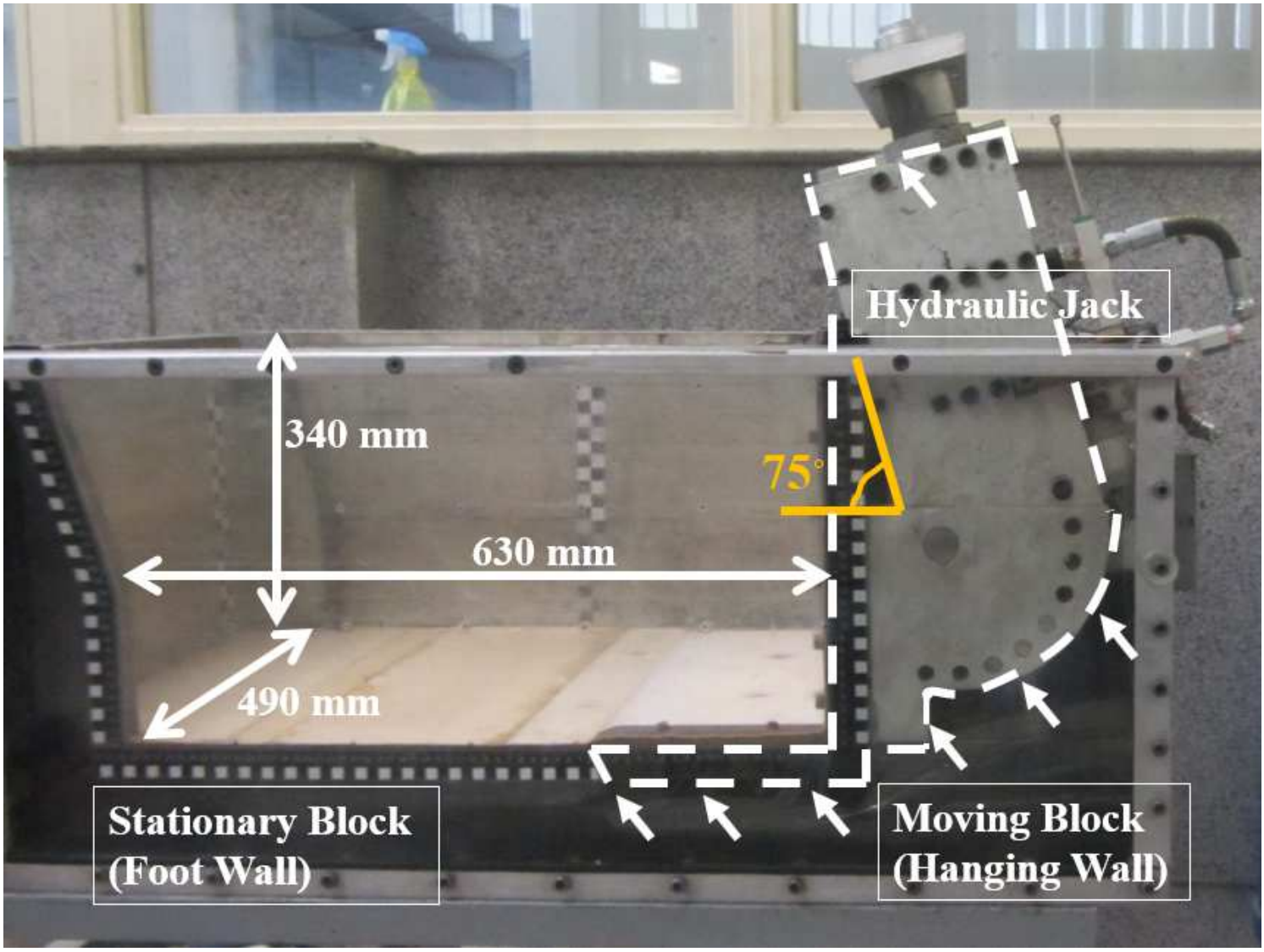

Figure 4

Centrifugal fault rupture simulation apparatus and its dimension

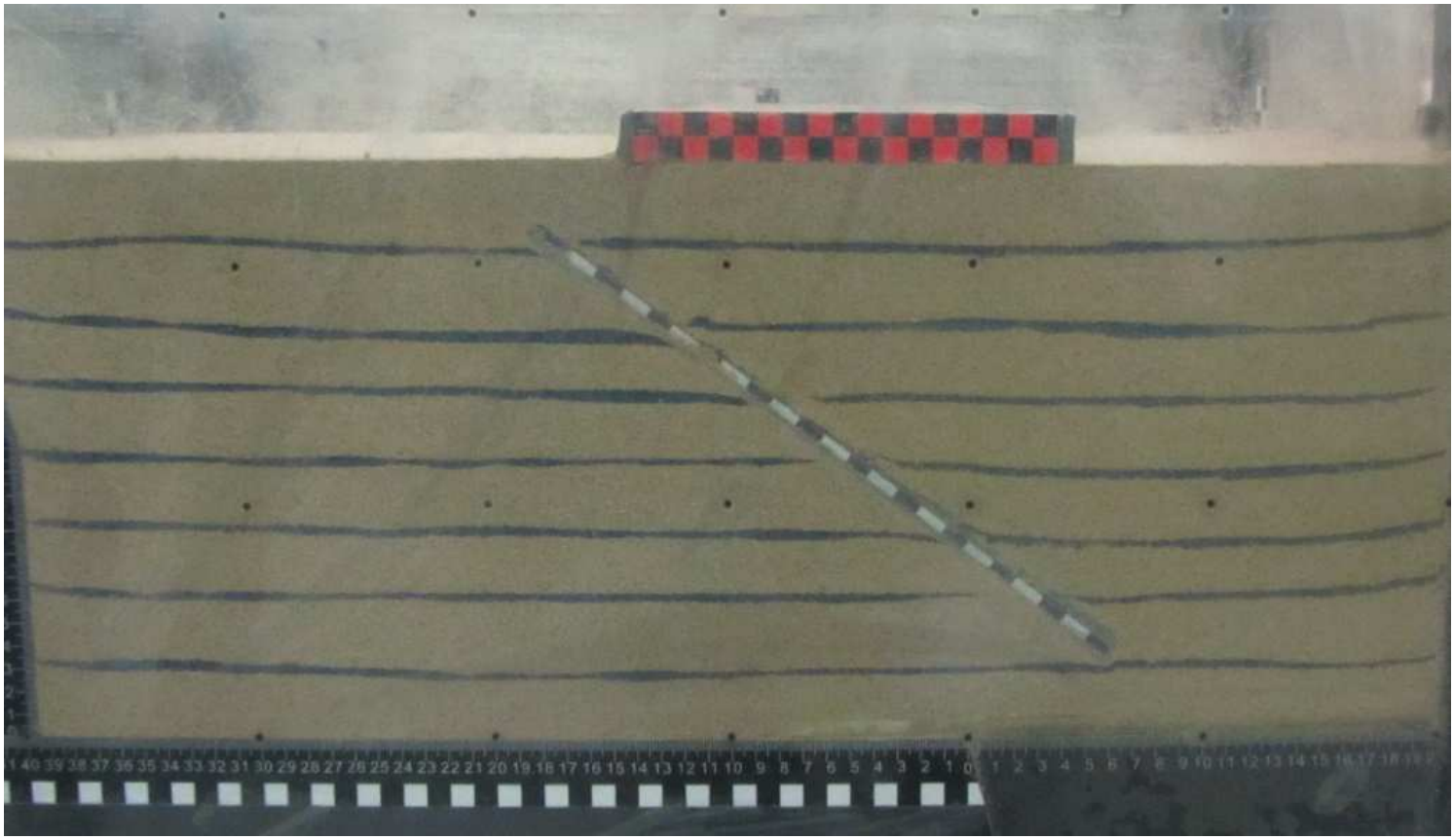

Figure 5

Centrifuge model inside the spilt box including both surface foundation and strong inclined wall

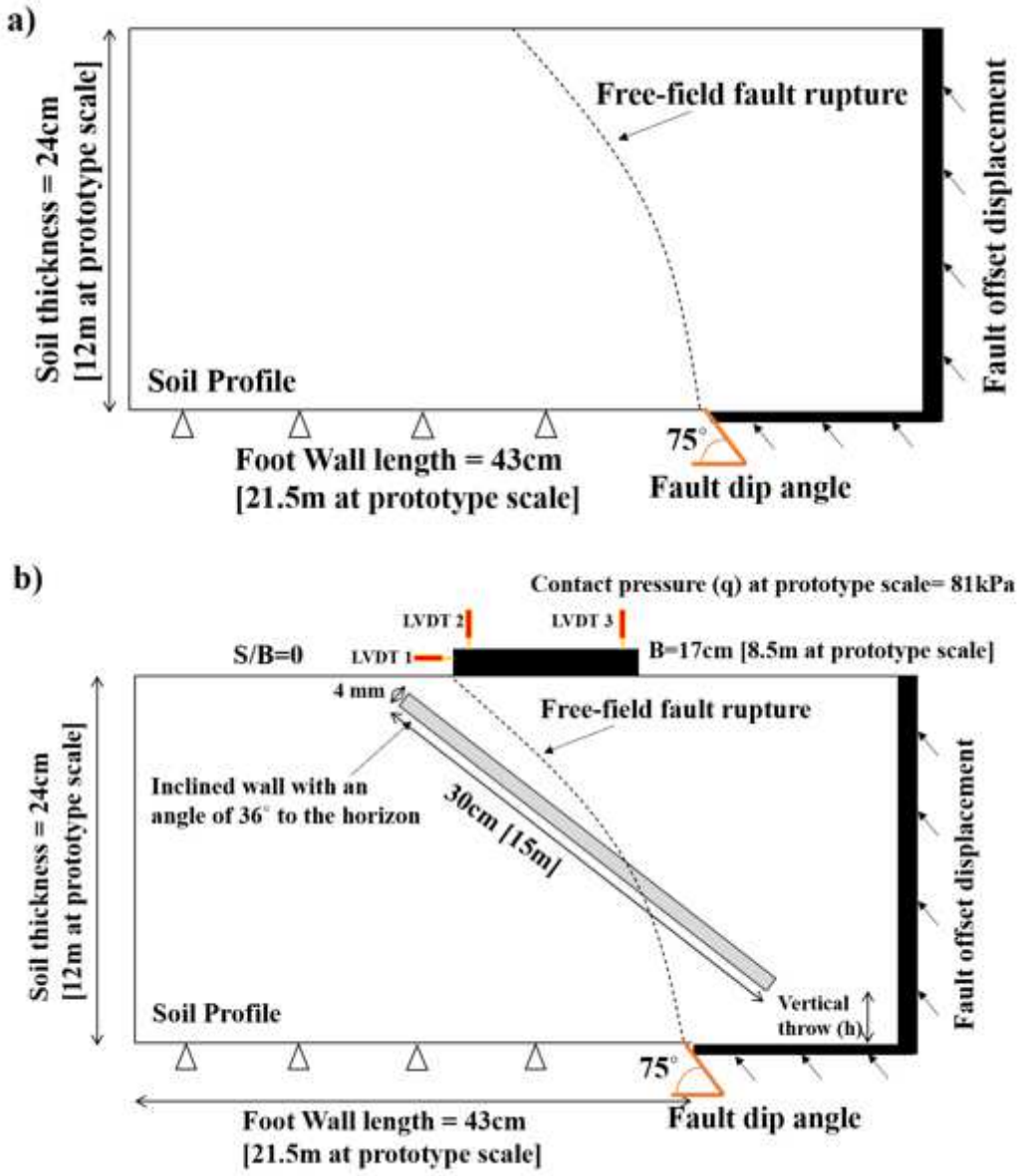

Figure 6

Schematic view of centrifuge experiments; (a) First test conducted to observe the free-field fault rupture, (b) second test to observe the practicability of implementing an inclined wall

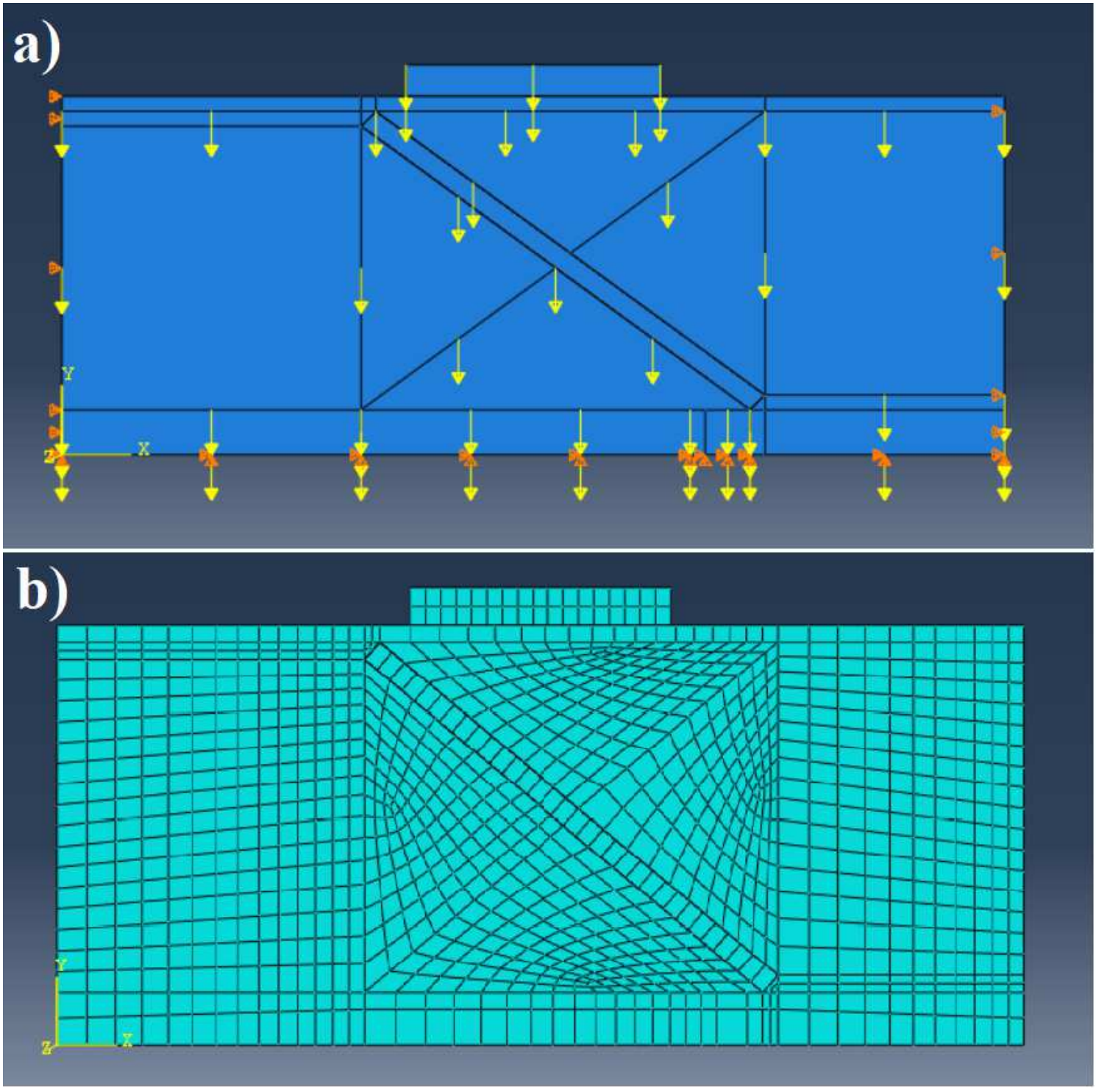

Figure 7

Two-dimensional Finite Element modeling; (a) boundary conditions, (b) meshing

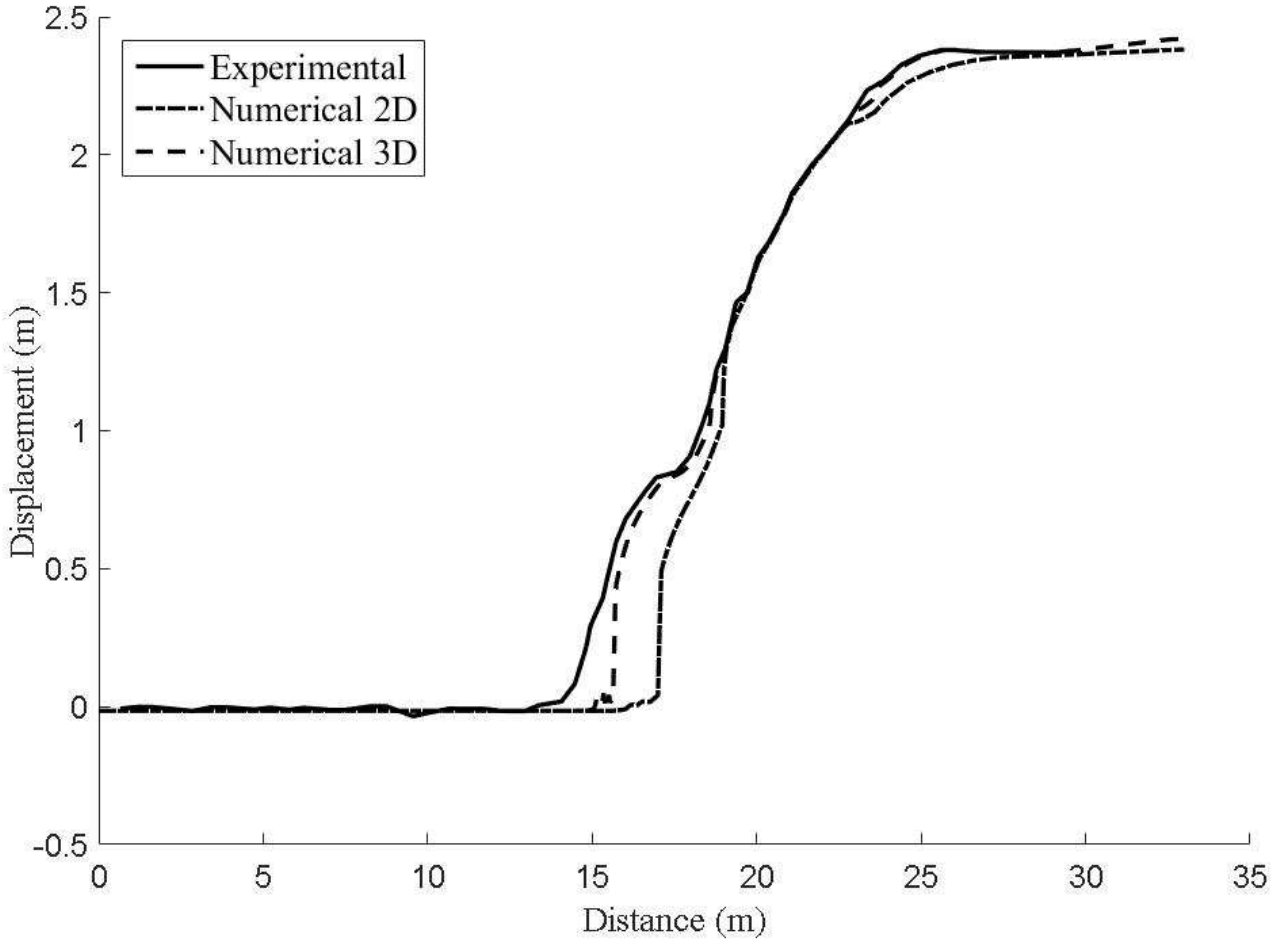

Figure 8

Vertical displacement of the surface when the fault throw is 2.4 m, both Experimental and Numerical results

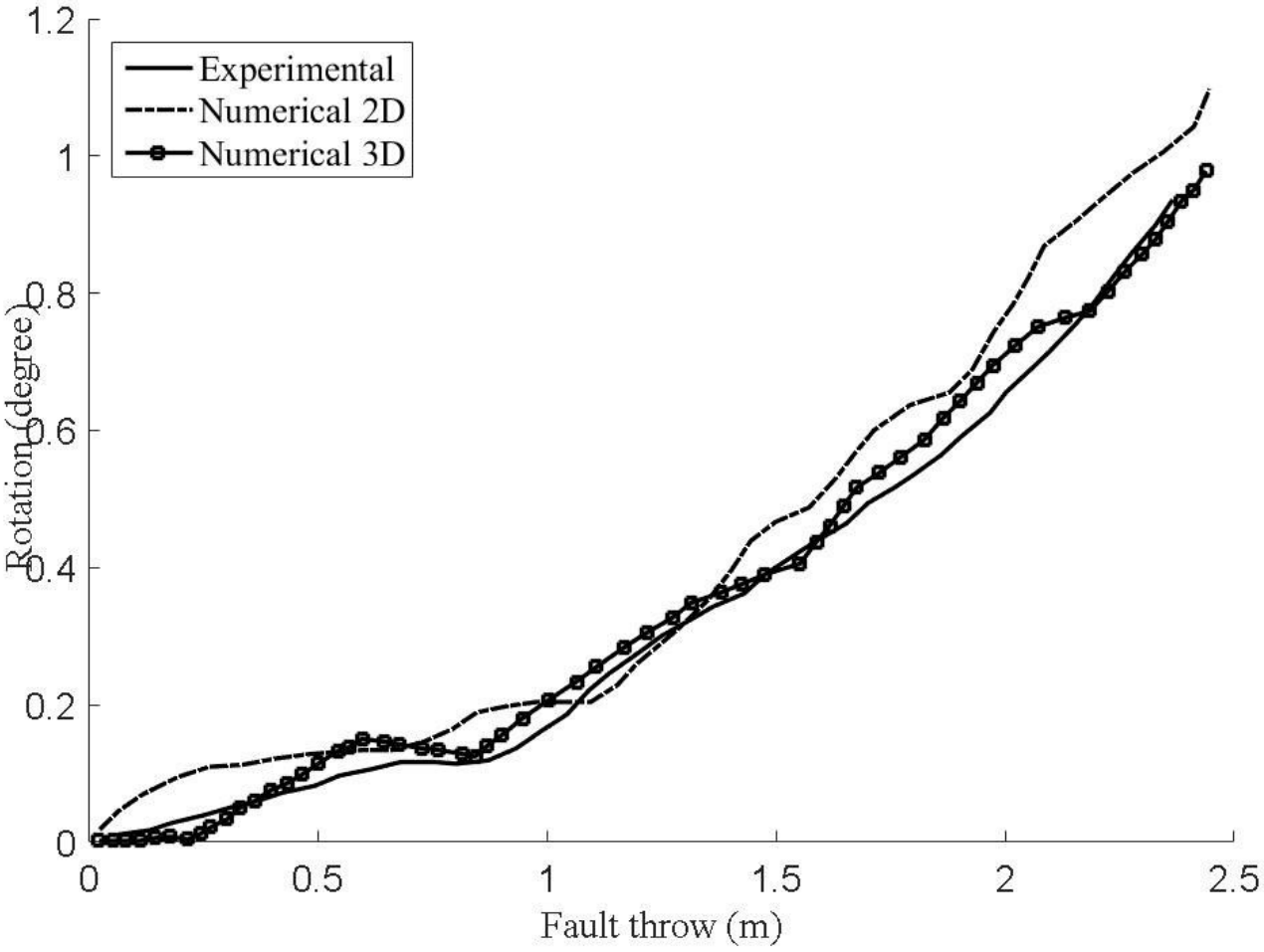

Figure 9

Rotation of surface foundation locating at S/B=0 versus vertical throw of the fault

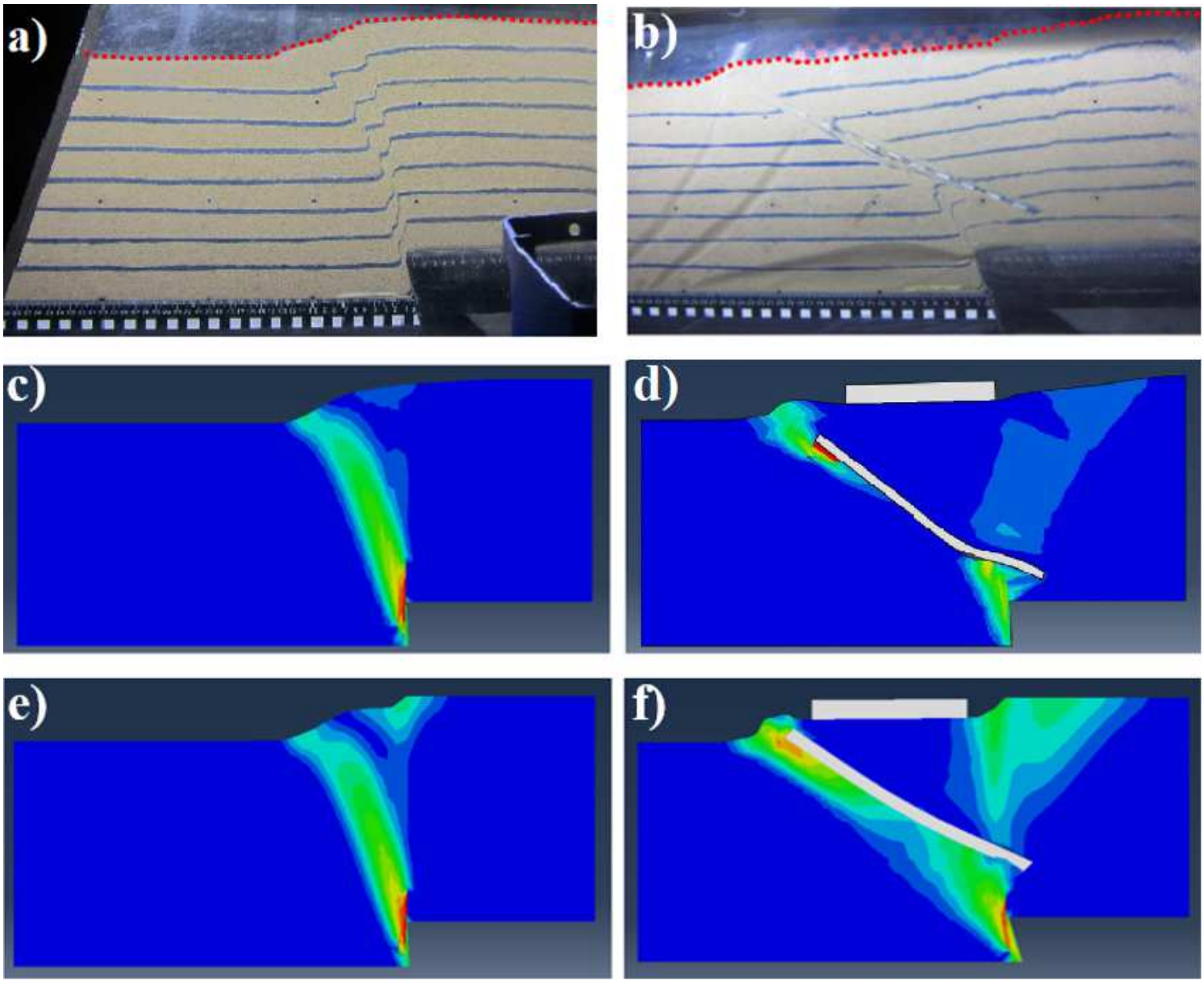

Figure 10

Comparison between the centrifuge experiments and both 2-Dimensional and 3-Dimensional numerical analysis; (a) centrifuge model for the free-field condition; (b) centrifuge model for the test with an inclined wall when a surface foundation was positioned at S/B=0; (c) the 2-Dimensional deformed mesh with plain strain contours for the free-field condition in finite element analysis; (d) the 2-Dimensional deformed mesh with plain strain contours for the test with an inclined wall when a surface foundation was positioned at S/B-0; (e) the 3-Dimensional deformed mesh with standard 3D stress for the free-field condition; (f) the 3-Dimensional deformed mesh with standard 3D stress for the test with an inclined wall when a surface foundation was positioned at S/B=0.

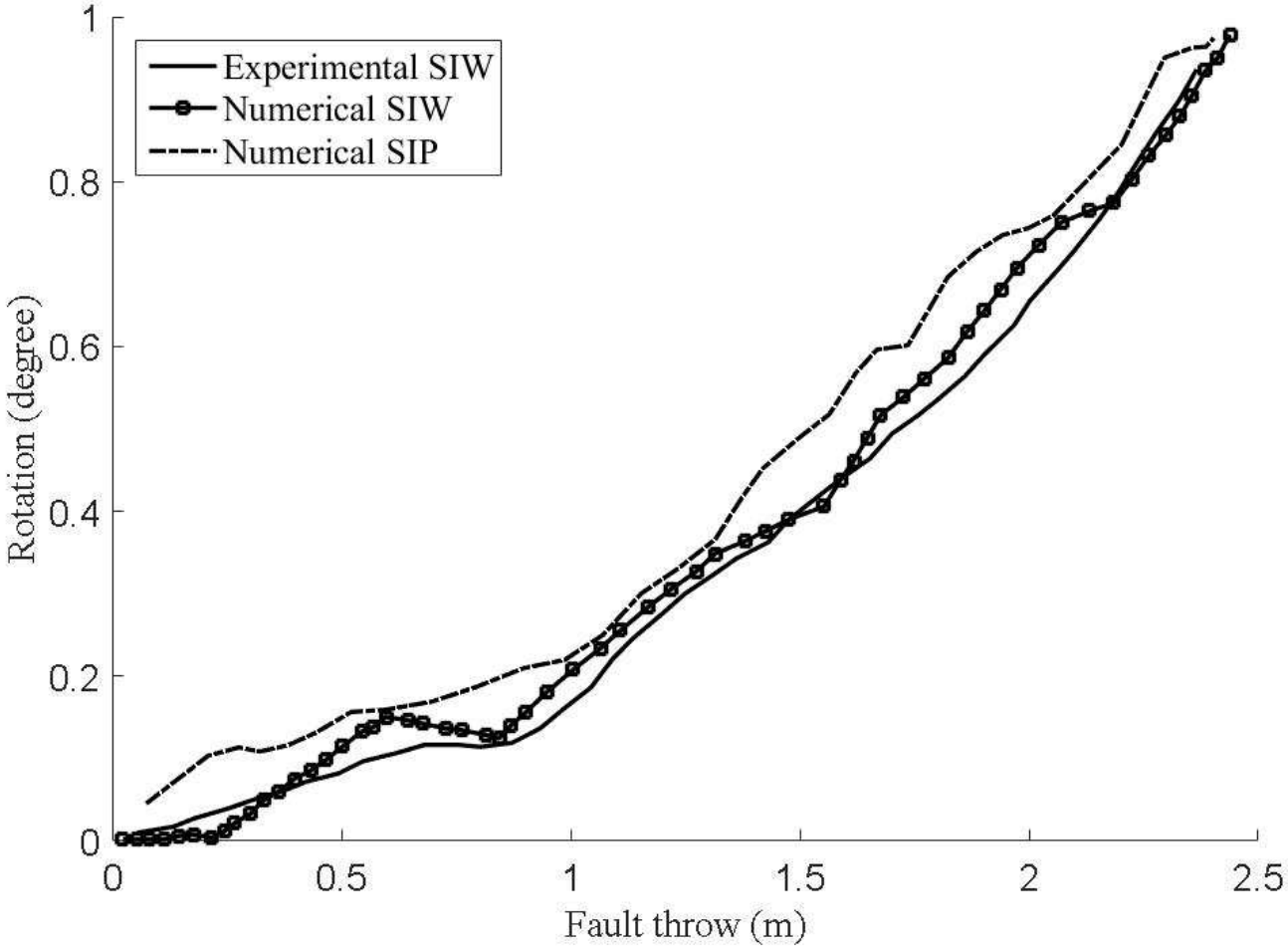

Figure 11

Rotation of surface foundation protected by both SIW and tangential SIMPs versus vertical throw of the fault

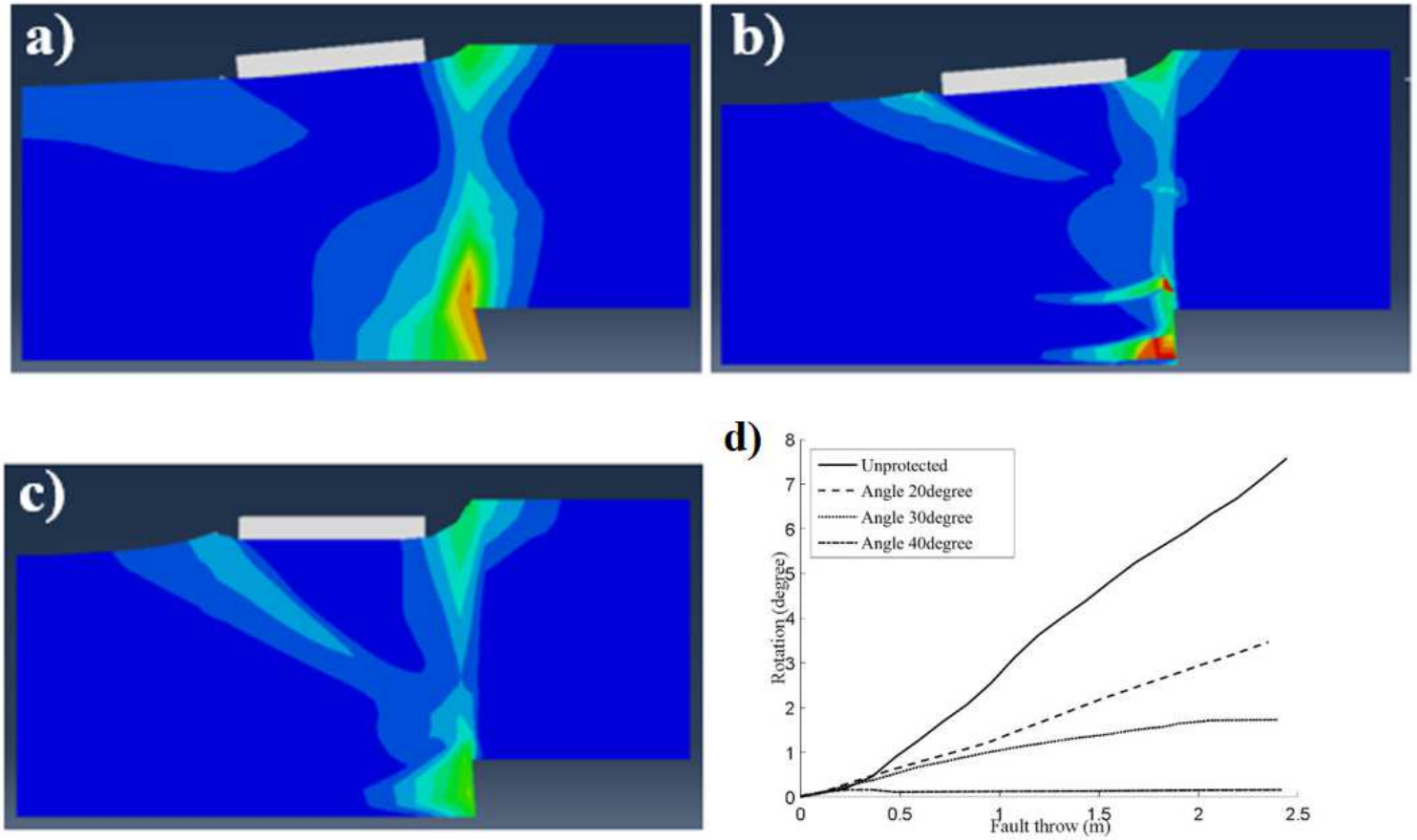

Figure 12

The effect of inclination on micro-piles; (a) inclined micro-piles of 20-degree; (b) inclined micro-piles of 30-degree; (c) inclined micro-piles on 40-degree; (d) the amount of rotation of the protected surface foundation

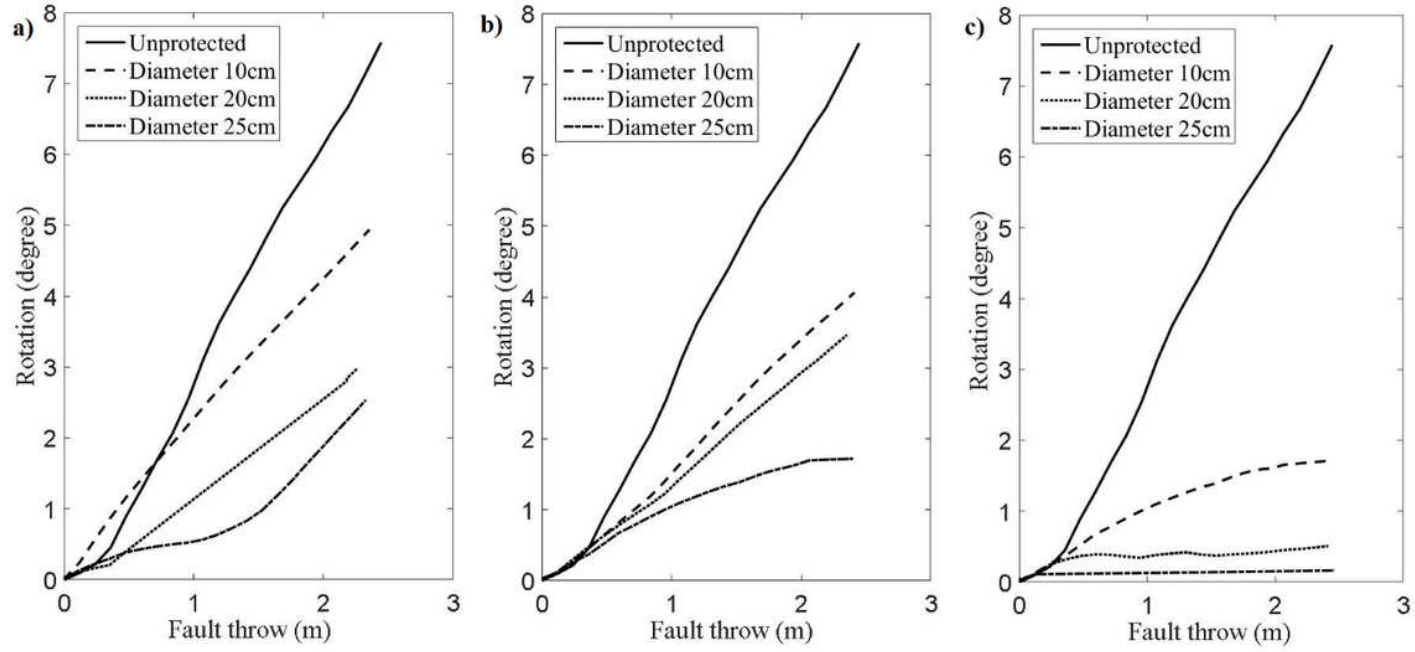

Figure 13

The effect of diameter on SIMPs when they are located with 50cm placing between every two consecutive micro-piles; (a) inclination angle of 20degree; (b) inclination angle of 30degree; (c) inclination angle of 40degree.

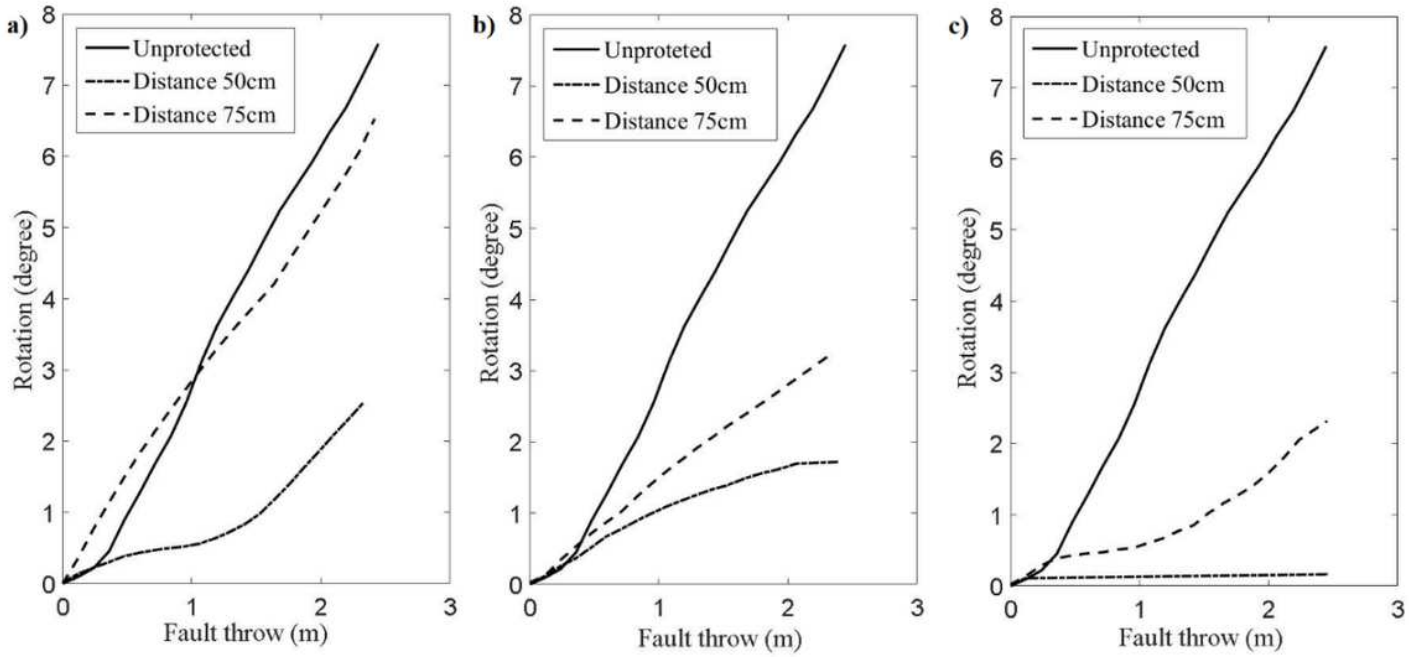

Figure 14

surface foundation rotation versus fault throw, when the foundation is protected by SIMPs with installation angle of (a) 20degree, (b) 30degree, (c) 40degree

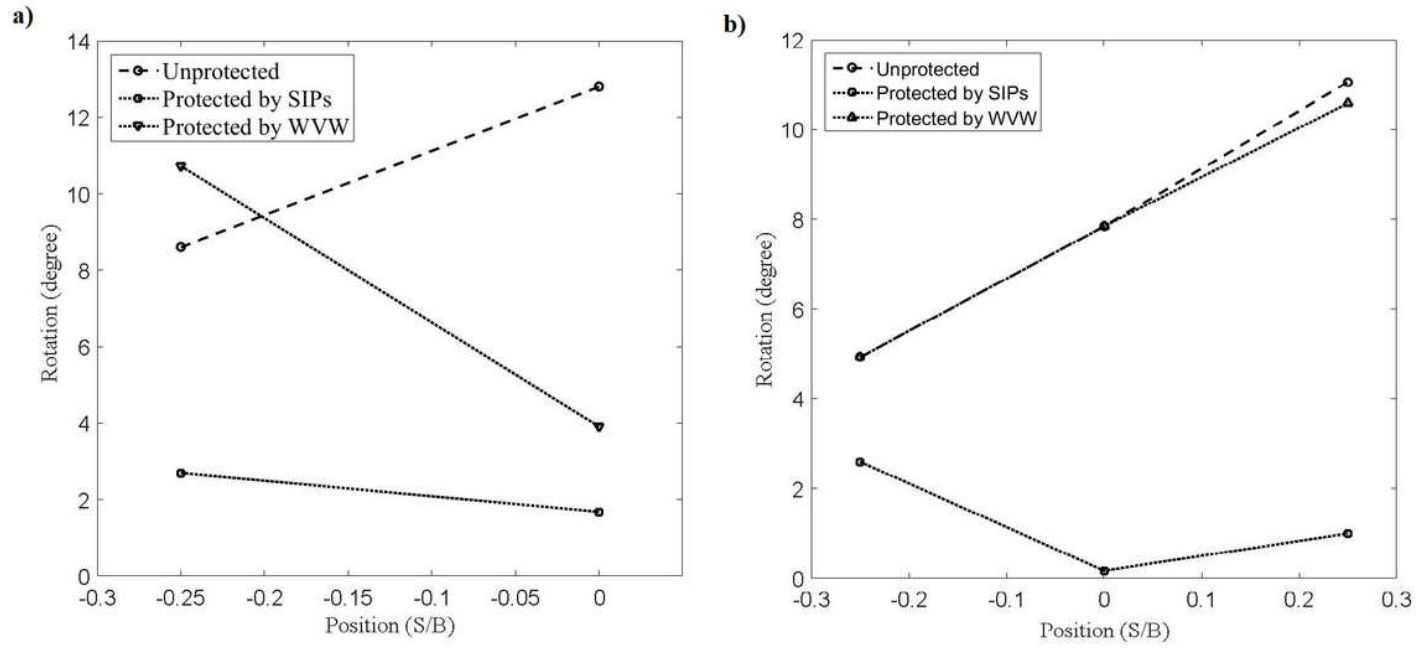

Figure 15

Effectiveness of conducting either SIMPs or a Weak Vertical Wall (WVW) to protect surface foundation against fault rupture of dip angle (a) 60degree, (b) 75degree.

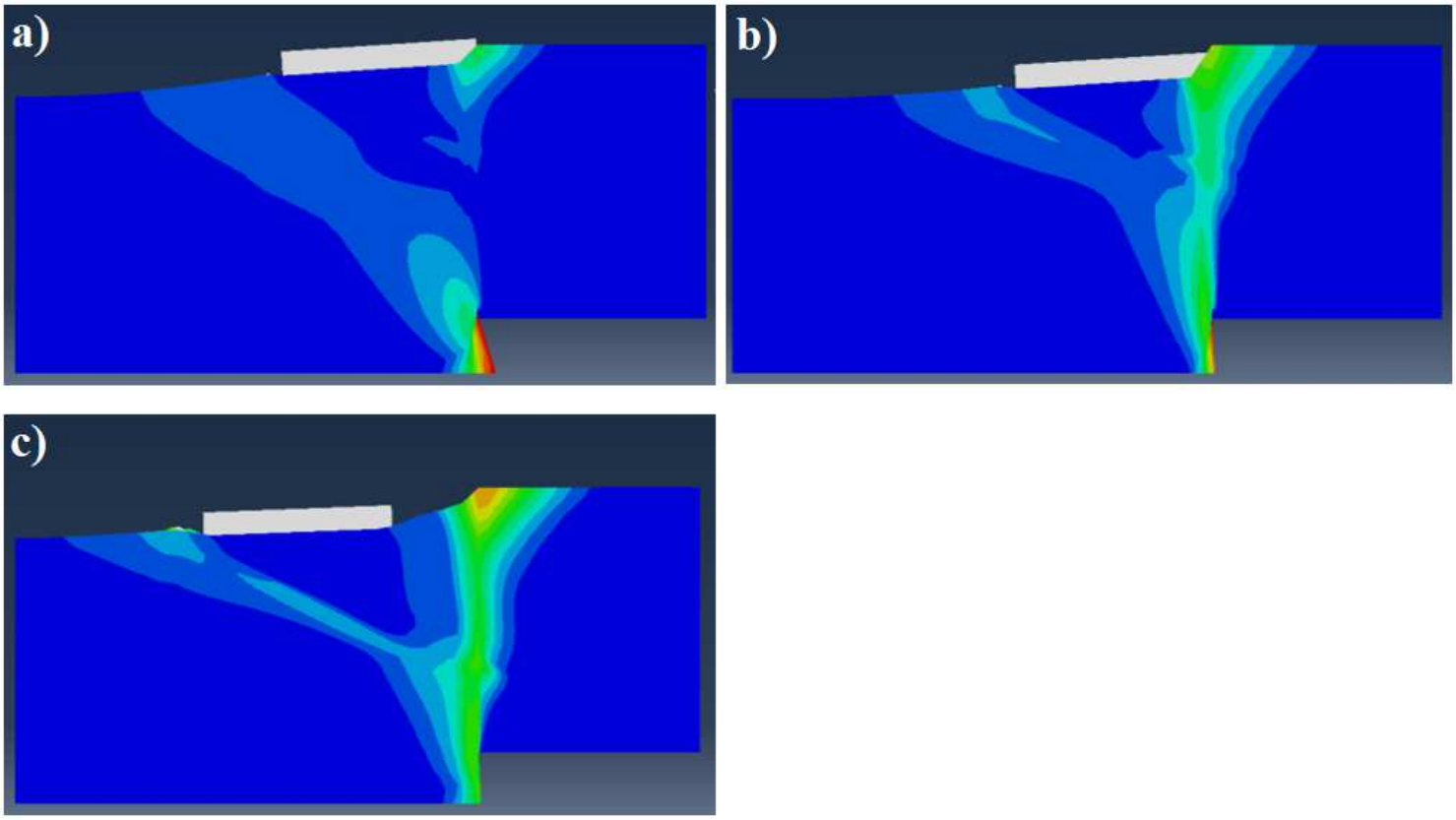

Figure 16

Numerical results of how a row of SIMPs affect the rotation of a surface foundation which is placed at (a) S/B=-0.25 against fault rupture of dip angle 60degree, (b) S/B=-0.25 against fault rupture of dip angle 75degree, (c) S/B=+0.25 against fault rupture of dip angle 75degree.